The Abdus Salam
International Centre for Theoretical Physics

2218-9

Mediterranean School on Nano-Physics
held in Marrakech - MOROCCO

2 - 11 December 2010

Optical and Electronic Properties of Impurities in Quantum Dot

ZORKANI Izzedine
Dep. de Physique, Faculte' de Sciences Dhar Mehraz
B.P.1796, Fes
MOROCCO

OPTICAL AND ELECTRONIC PROPERTIES OF IMPURITIES IN QUANTUM DOT

Izeddine Zorkani

Dep. de Physique, Faculté des Sciences Dhar Mehraz, B.P.1796, Fes-Morocco

Groupe des Nanomateriaux et Energies Renouvelables, FSDM, FES-Morocco.

http://www.fsdmfes.ac.ma

OUTLINE

- **INTRODUCTION to Nanotechnology, MOTIVATION FOR: QD**
- **Impurity State (HEMT)**
- **From Quantum Well to Quantum Dots**
- **Effects of a Magnetic field:**
  - Absorption Coefficient of *Magneto-Donor in a QD*
  - Polarizability of M*agneto-Donor in a QD*
  - Polaronic effects
  - Absorption Coefficient of *Magneto-Polaron in a QWWire*
- **CONCLUSION**

10 mm	Chip
1 mm	Grain of sand
100 µm	Hair wire diameter
10 µm	Transistor in a integrated circuit
1 µm	Smoke particle
100 nm	TiO_2 pigment particle
10 nm	Gold nanocrystal containing 30 0000 atoms
1 nm	DNA molecule width
0.1 nm	*C-C* bond lenght in ethine

By Tito Trindade, University of Aveiro, 2002 , Portugal

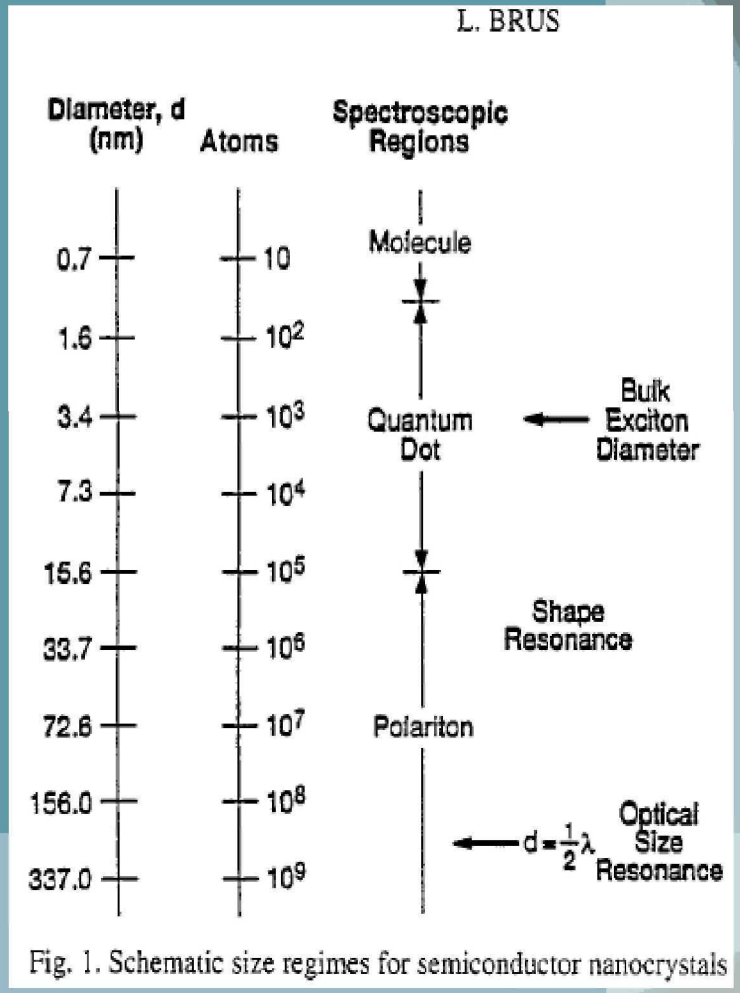

Fig. 1. Schematic size regimes for semiconductor nanocrystals

From: L.Brus, J.Phys.Chem.Solids (1998)

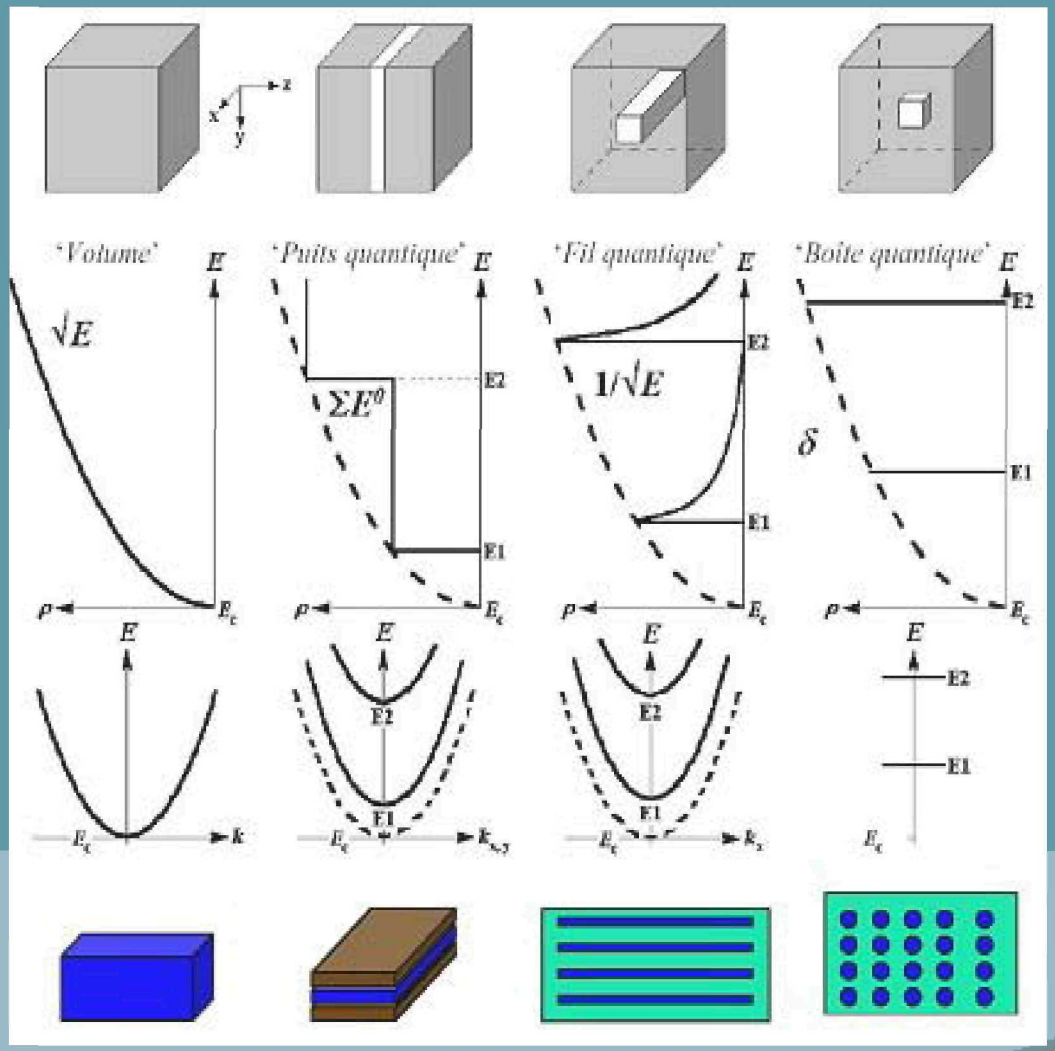

- *Density of states as the dimensionality of the structure reduces from 3D (bulk) to 0D (quantum dot).*

SIZE EVOLUTION OF THE DENSITY OF ELECTRONIC STATES IN NANOCRYSTALS

- A defining characteristic of the modern view of atoms is that electronic energy levels are discrete and well separated.
- In contrast, the electronic levels in crystalline solids are diffuse bands of states.
- In nanometer-size crystals, the density of electronic energy levels varies smoothly between the atomic and bulk limits

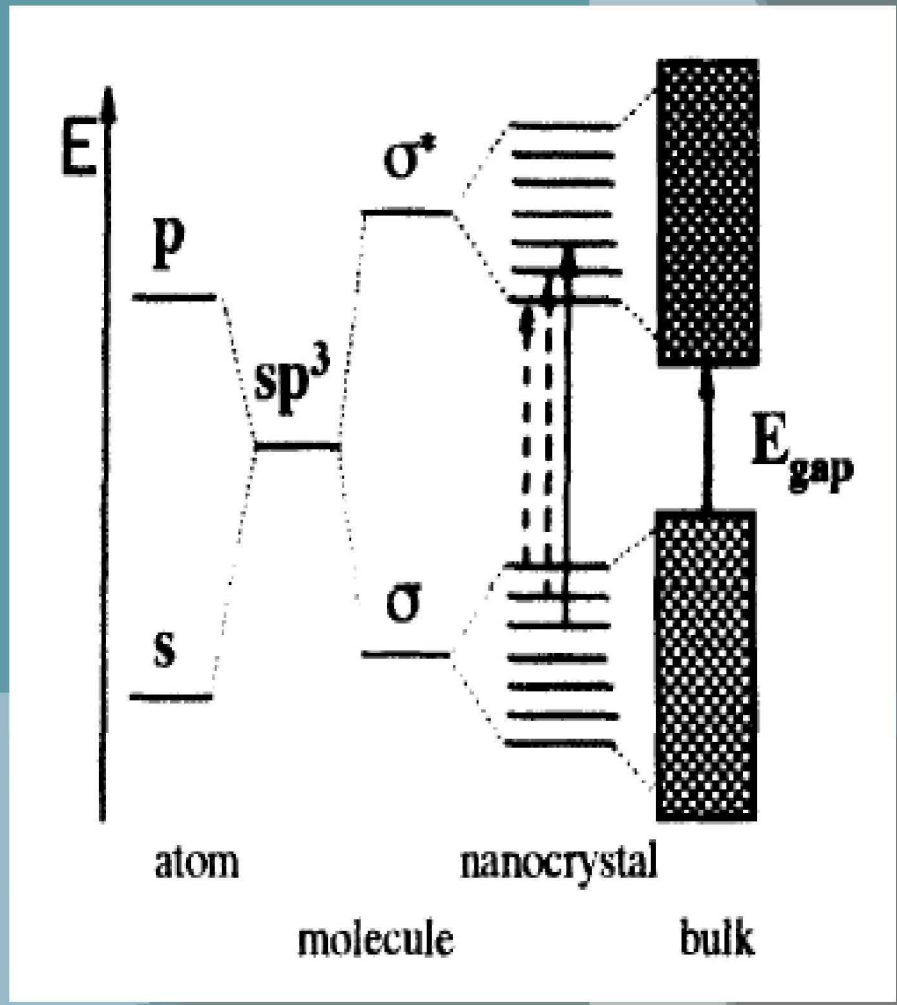

from A.P. Alivisatos,1997

DOPING: DONOR IMPURITIES

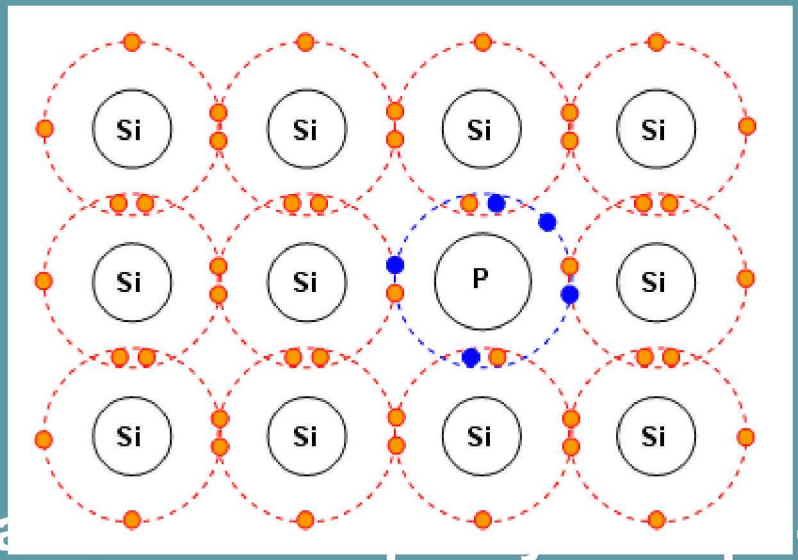

Silicon la… orus atom added:

- Compared to Si, Phosphorus has one extra valence electron
- The extra valence atom is weakly bond to the P atom: an energy E_i=**Ec-Ed<< Eg is required to create a free electron from an impurity atom**
- This type of impurity is called **donor impurity**

DOPING: ACCEPTOR IMPURITIES

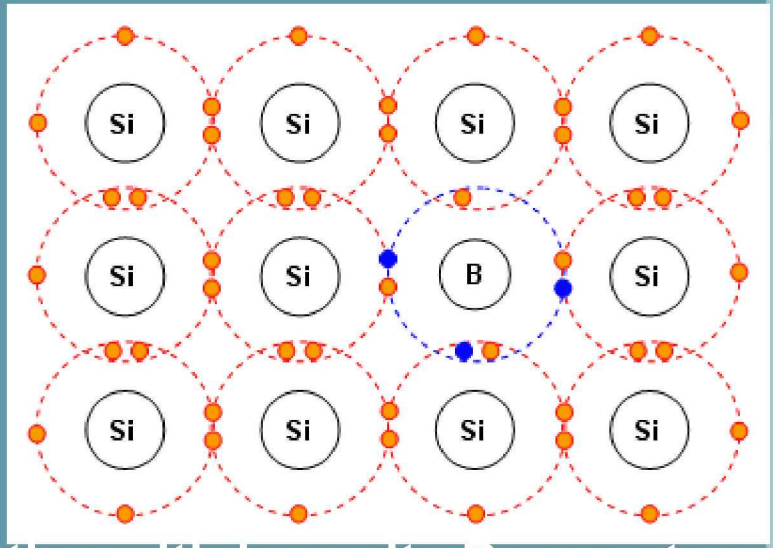

Silicon lattice with impurity Boron atom added:

- Boron has one valence electron less than the Si atom.
- An energy $E_i = Ea - Ev << Eg$ is required for an electron in the valence band to fill the excess hole induced by the B atom. This transition creates a holein the valence band.
- This type of impurity is called acceptor impurity.

Hydrogenic Effective Mass Theory (HEMT)

L'équation de Schrödinge régissant le mvt du Donneur dans le potentiel Coulombien s'écrit:

$$\left(-\frac{\hbar^2}{2m^*}\nabla^2-\frac{e^2}{\varepsilon r}\right)F(\vec{r})=EF(\vec{r})$$

$$E_n=-\frac{R^*}{n^2}$$

$$R^*=-\frac{m^*e^4}{2\hbar^2\varepsilon^2}$$

$$a^*=\frac{\hbar^2\varepsilon}{m^*e^2}=\varepsilon\frac{m}{m^*}a_0$$

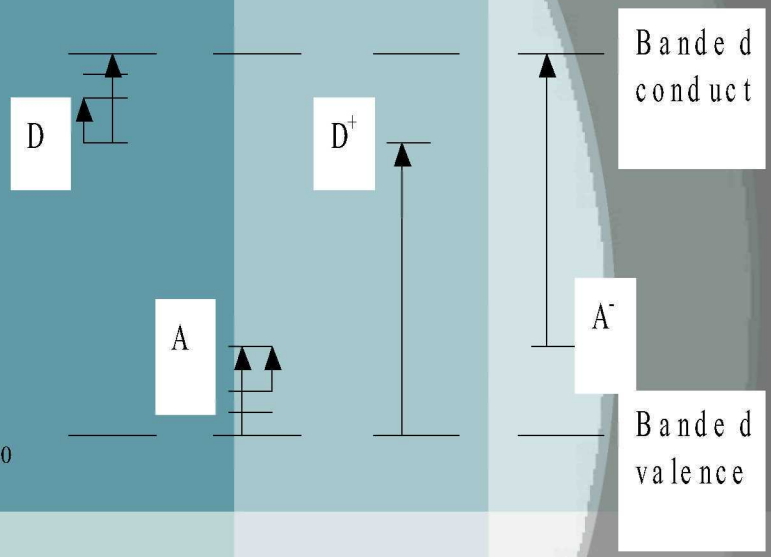

$$F_{1s}(\vec{r})=\frac{1}{\sqrt{\pi a^3}}\exp\left(-r/a^*\right)$$

L'énergie d'ionisation dépend de la nature chimique du semiconducteur mais pas celle de l'impureté

III

ZnSe : Al
ZnSe : Ga
ZnSe : In

expériences !

	th.	Al	Ga	In
ZnSe	24.522	26.3	27.9	28.9

E_∞
m^*

	th.	Sn	Si	O	
GaP Donneur	37.0	65.5	82.1	895	Donneurs dans GaP.
		C	Zn	Ge	
GaP Accepteur	42.5	48.0	64.0	258	Accept. dans GaP.

Tableau 2.2. : Energies d'ionisation dans le ZnSe et de donneurs et accepteurs dans le GaP. Les valeurs expér. sont comparées aux valeurs th. L'unité est le mev. Cfr réf. 8 et 9.

TME (même des versions plus évoluée) : incapable de rendre compte du "Déplacement Chimique"

REMEDE : Modèle simple (sans calcul de bande)

$$V_I(r) = -\frac{e^2}{\varepsilon_\infty r}$$

ε_∞ : Constante diélectrique (facteur d'écran)

Tient compte de la relaxation de la densité de charge autour de l'impureté $\varepsilon_\infty \longrightarrow \varepsilon_\infty(q)$

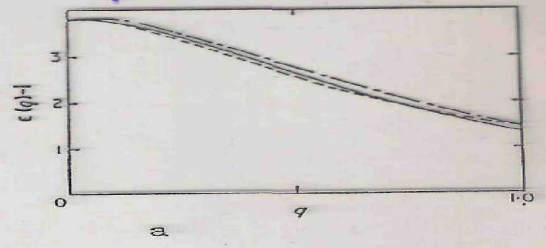

a

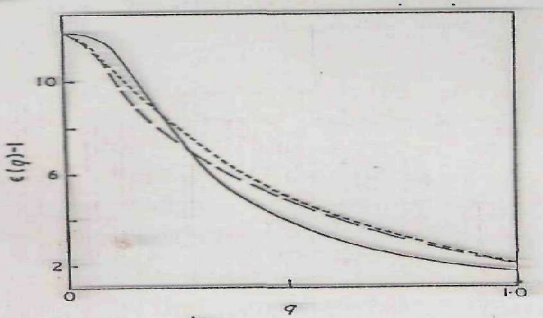

b

ZnS

Fig. 2.6. : Courbes théoriques de $\varepsilon_\infty(\vec{q})-1$ en fonction de $\vec{q}$, pour ZnS (a) et InAs (b) dans les directions de symétrie

111 (————),
200 (——·——·——),
220 (— — —).

Nous ajustons la forme analytique (2.14) à ces courbes théoriques déterminées par Vindsome et Richardson [11].

* Lorentzienne (Forme Analytique) :

$$\frac{1}{\varepsilon_\infty(q)} = \frac{1}{\varepsilon_\infty}\left[1 + \frac{Aq^2}{B+q^2}\right]$$

$\lim_{q \to 0} \varepsilon_\infty(q) = \varepsilon_\infty$

$\lim_{q \to \infty} \varepsilon_\infty(q) = 1$

On pose : $B = K^2$

$$\varepsilon_\infty(q) = \varepsilon_\infty \frac{q^2 + K^2}{\varepsilon_\infty q^2 + K^2}$$

↓ T-F $\quad \left(V(r) = -4\pi e^2 \int \frac{d\vec{q}\, e^{i\vec{q}\cdot\vec{r}}}{\varepsilon(q)\cdot q^2}\right)$

$$V_I(r) = -\frac{e^2}{\varepsilon_\infty r}\left[1 + (\varepsilon_\infty - 1)e^{-Kr}\right]$$

* Tient Compte de la différence entre l'ion de l'impureté et celui qu'il remplace :

$\frac{\delta}{2} r e^{-\delta r}$

$K(Si) = 1.755\ \text{Å}^{-1}$

$$V_I(r) = -\frac{e^2}{\varepsilon_\infty r}\left[1 + (\varepsilon_\infty - 1)\left(e^{-Kr} + \frac{\delta}{2} r e^{-\delta r}\right)\right]$$

Exciton: bound electron-hole pair (EHP)

Dans un cristal massif, l'énergie et la fonction d'onde enveloppe de l'exciton sont solutions de l'équation suivante

$$\left(-\frac{\hbar^2}{2m_e^*}\nabla_e^2-\frac{\hbar^2}{2m_h^*}\nabla_h^2-\frac{e^2}{\varepsilon\left|\vec{r}_e-\vec{r}_h\right|}\right)F\left(\vec{r}_e,\vec{r}_h\right)=EF\left(\vec{r}_e,\vec{r}_h\right)$$

$$\vec{R}=\frac{m_e^*\vec{r}_e+m_h^*\vec{r}_h}{m_e^*+m_h^*} \qquad \vec{r}=\vec{r}_e-\vec{r}_h$$

$$\left(-\frac{\hbar^2}{2M}\nabla_R^2-\frac{\hbar^2}{2\mu}\nabla_r^2-\frac{e^2}{\varepsilon r}\right)F\left(\vec{R},\vec{r}\right)=EF\left(\vec{R},\vec{r}\right)$$

Aux différents valeurs de n correspondent les niveaux d'exciton:

$$E_n=-\frac{\mu e^4}{2\varepsilon^2\hbar^2}\frac{1}{n^2} \qquad E_{ex}=-\frac{\mu e^4}{2\varepsilon^2\hbar^2}$$

Quantum Wells

- QWs are formed from multiple heterojunctions. If a thin layer of a narrower-bandgap material ‘B’ is sandwiched between two layers of wider-bandgap material ‘A’, then they form a double heterojunction.

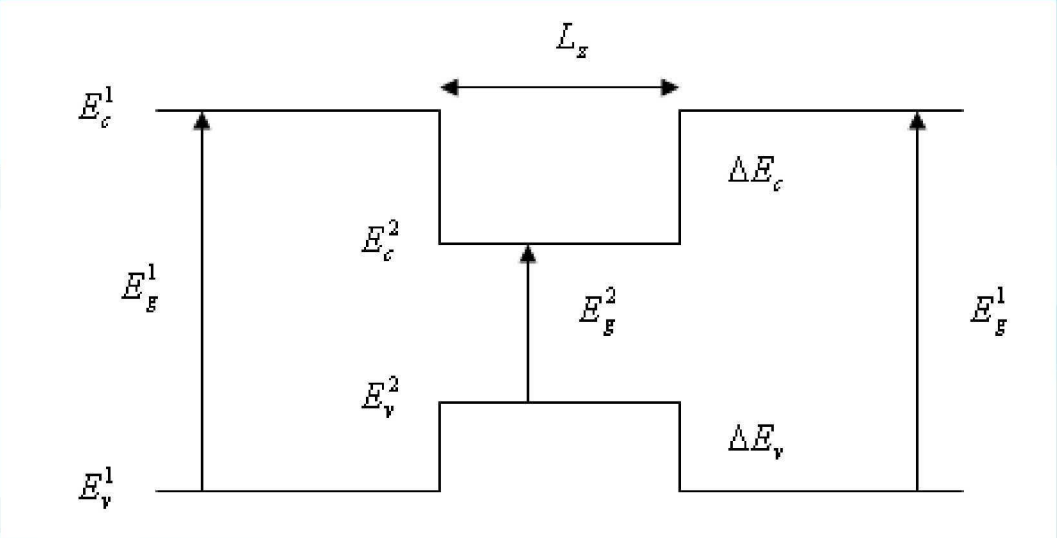

Particle in a QW

$$\left(-\frac{\hbar^2}{2m^*}\nabla^2 + V_w(z)\right)F(\vec{r}) = EF(\vec{r})$$

$$V_w(z) = \begin{cases} 0 & pour \quad |z| < \frac{L_z}{2} \\ V_0 & pour \quad |z| > \frac{L_z}{2} \end{cases}$$

For the even solutions we have

$$f_n(z) = \begin{cases} A\cos(k\,z) & pour \quad |z| < \frac{L_z}{2} \\ B\exp(-\rho|z|) & pour \quad |z| > \frac{L_z}{2} \end{cases}$$

$$k = \sqrt{\frac{2m^* E_z}{\hbar^2}} \qquad \rho = \sqrt{\frac{2m^*(V_0 - E_z)}{\hbar^2}}$$

$$k\tan\left(k\frac{L}{2}\right) = \rho$$

$$\left|\cos\left(\frac{ka}{2}\right)\right| = \frac{k}{k_0} \qquad tg\left(\frac{ka}{2}\right) > 0$$

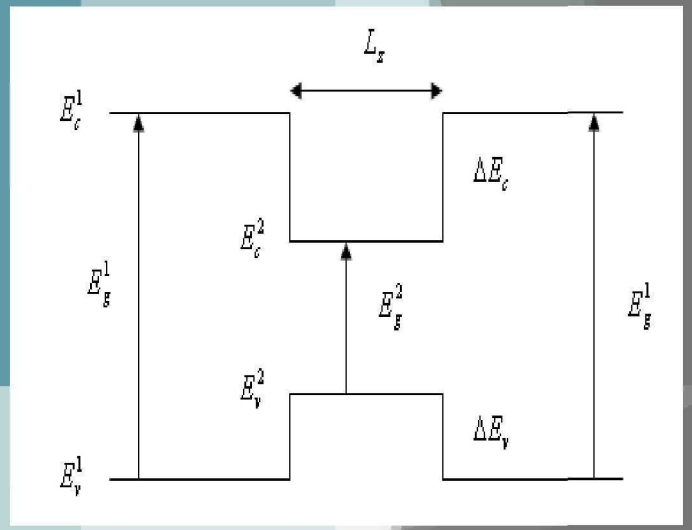

For the odd solutions we will have sin(kz)

Pour la résolution on utilise une méthode graphique: Solution par Ordinateur

```
> eq:=cos(abs(z))=z;

> plot({cos(abs(z)),z},z=0..Pi/2 );
```

$$eq := \cos(|z|) = z$$

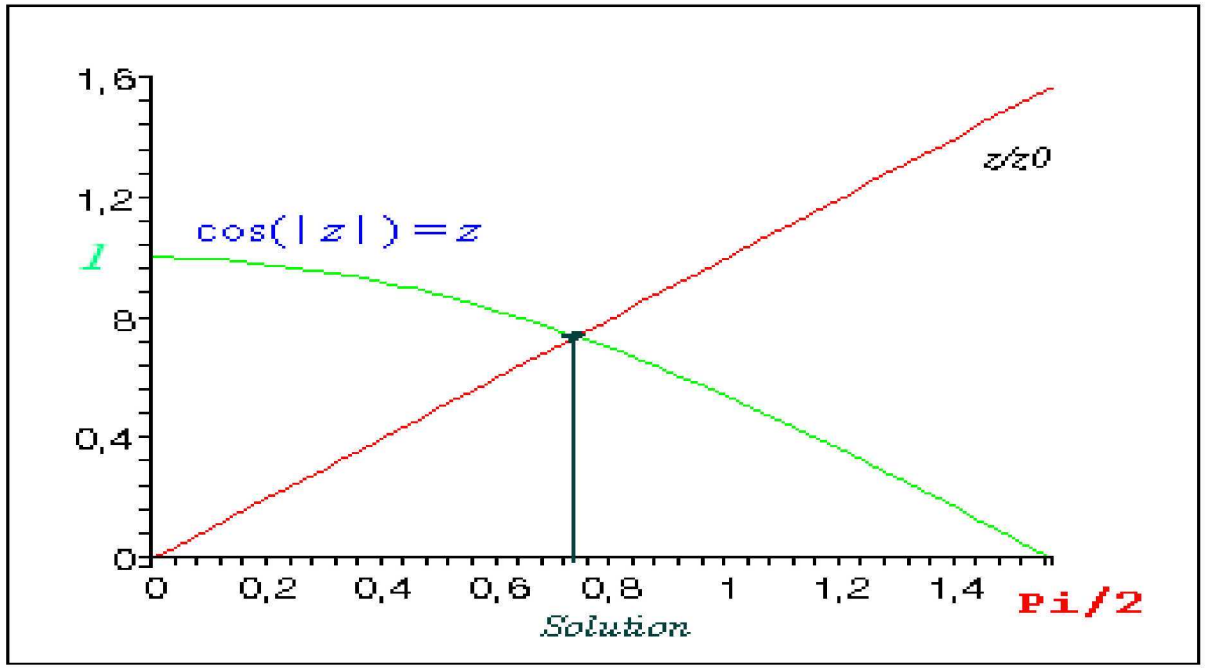

Quantum Confined Systems

Heterostructure Systems: Quantum Well (QW)

$\Delta E_c = f\Delta E_g$ empirically $f = 0.65$ for GaAs/AlGaAs

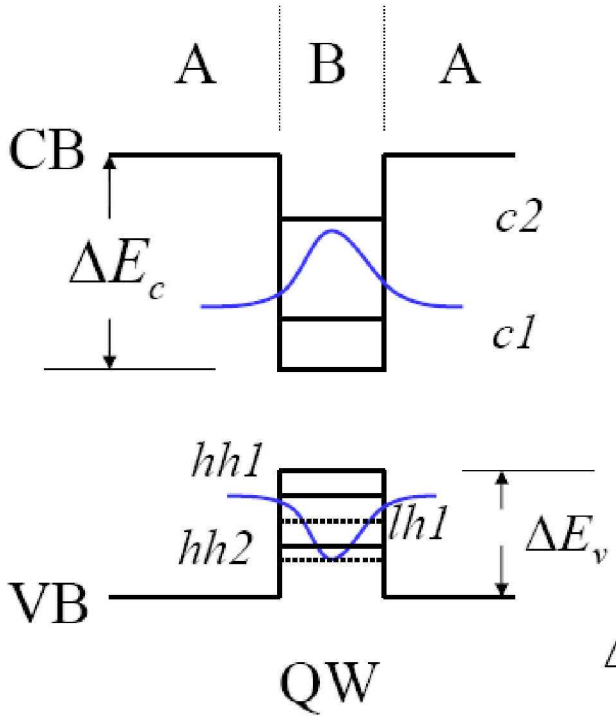

Each state (c1, c2, hh1, hh2, etc. corresponds to the formation of a two-dimensional subband, which is free electron like in plane parallel to well.

$$\Delta E_g = E_g^{AlGaAs} - E_g^{GaAs}$$

Quantum Wells

Quantum Confined Systems: Optical Properties

The effective bandgap in a QW system:

$$E_g = E_{gA} + E_1(electron) + E_1(heavy\ hole)$$

The effective bandgap will be larger than that of well material. It can be changed by varying the well width L_z. The blue shift of the effective bandgap is called *"quantum size effect"*.

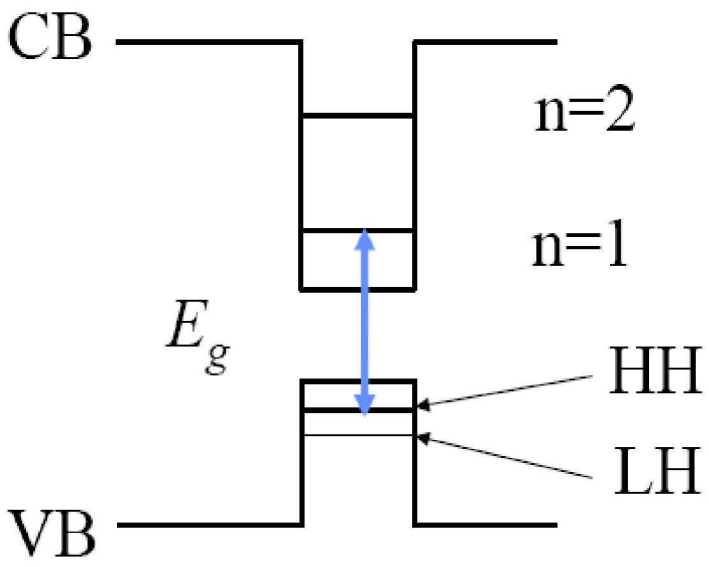

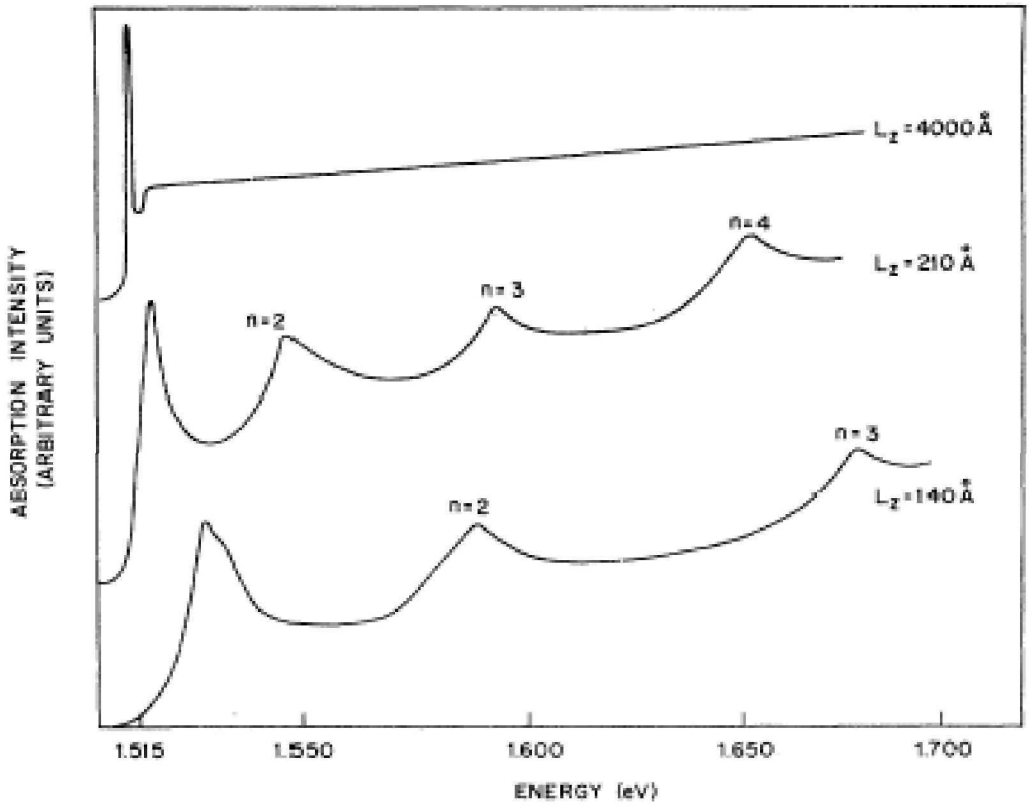

FIG. 2. Typical absorption spectra at 2 K. The traces labeled $L_z = 210$ Å and $L_z = 140$ Å show excitons associated with the electron and hole, each in the nth bound state. For $L_z = 4000$ Å, the absorption coefficient α (cm^{-1}) is about 2.5×10^4 at the exciton peak and $\approx 1 \times 10^4$ in the band-to-band region. Similar values are obtained for the thinner multilayers.

Optical absorption in Quantum Wells

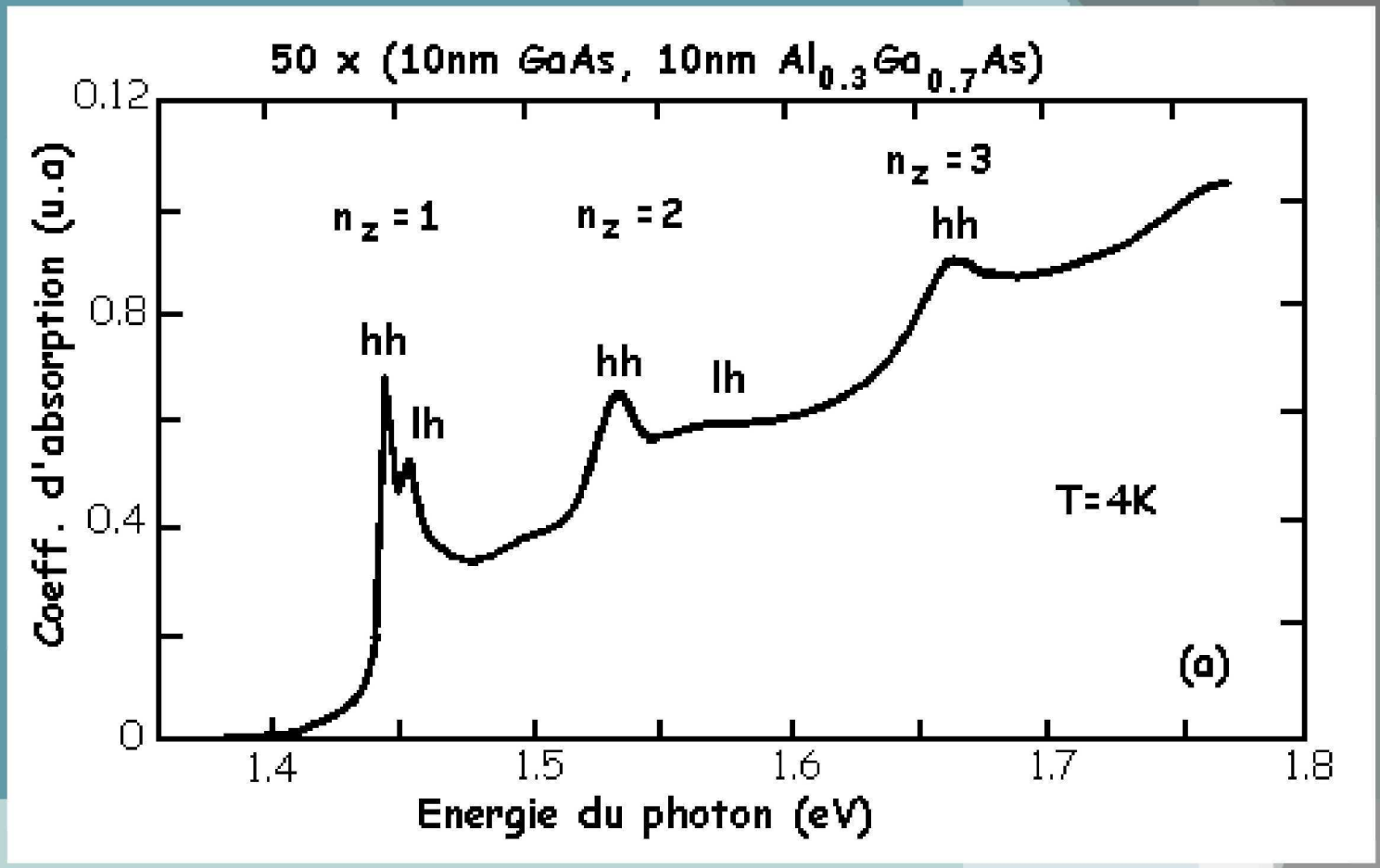

Spectre d'absorption à basse température d'un puits quantique multiple de GaAs/GaAlAs

Quantum Dot

- QD result of the nanocrystal being smaller than the bulk semiconductor Bohr exciton diameter.
- By forcing the electron and hole to occupy a space smaller than the normal equilibrium distance in the bulk material (dotted line), it takes more energy to promote the electron from the valance band to the conduction band
- Hence the smaller the nanocrystal is the larger the band gap of the material is and the bluer the emission from the nanocrystals is.
- Nanocrystals have mainly interesting properties resulting from quantum confinement effect
-

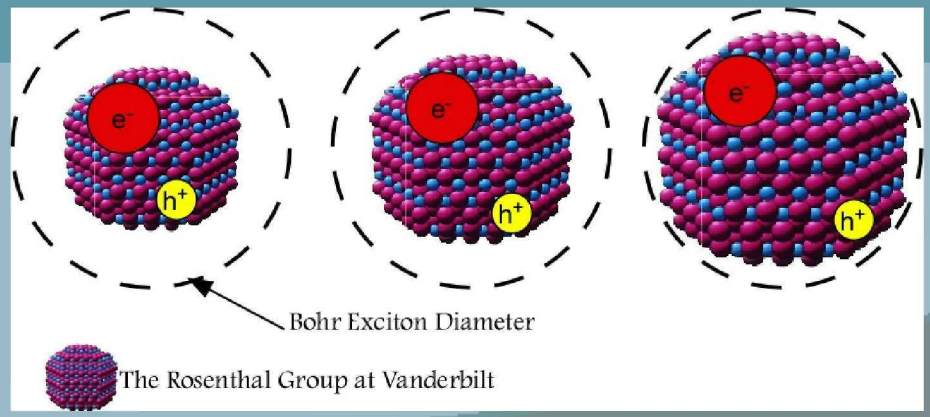

ELECTRONIC STATES IN NANOCRYSTALS

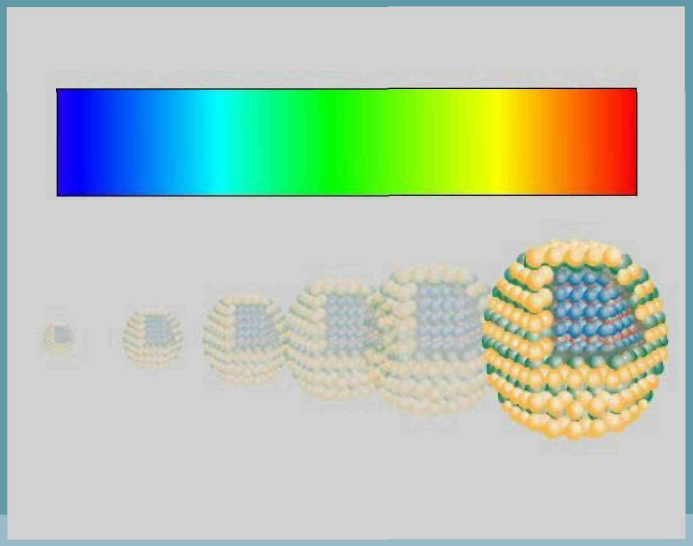

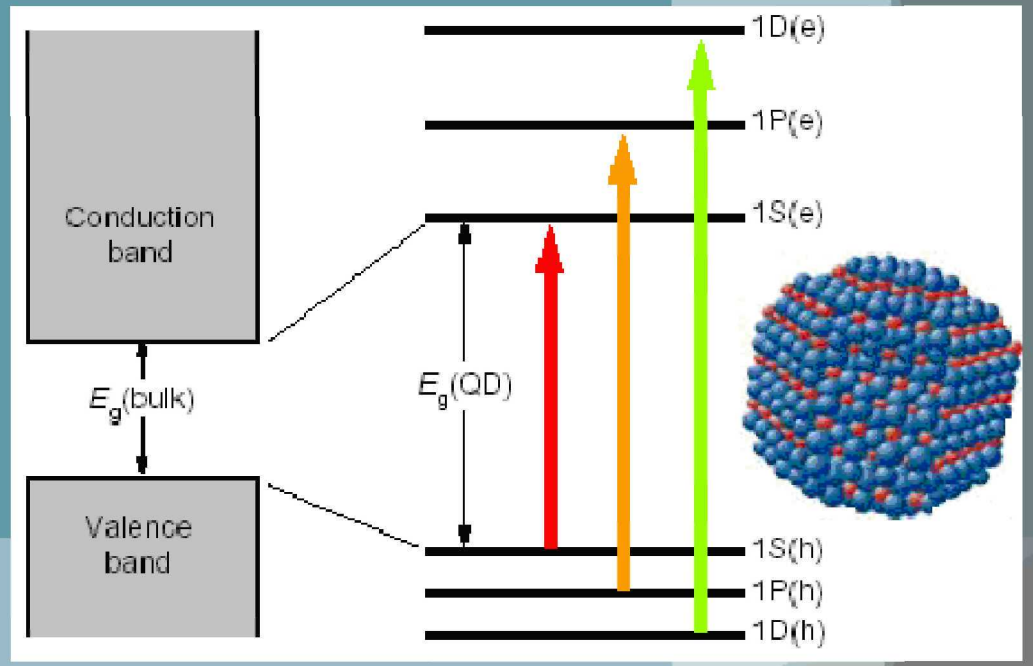

Bulk semiconductor QD (e : electron, h : hole).

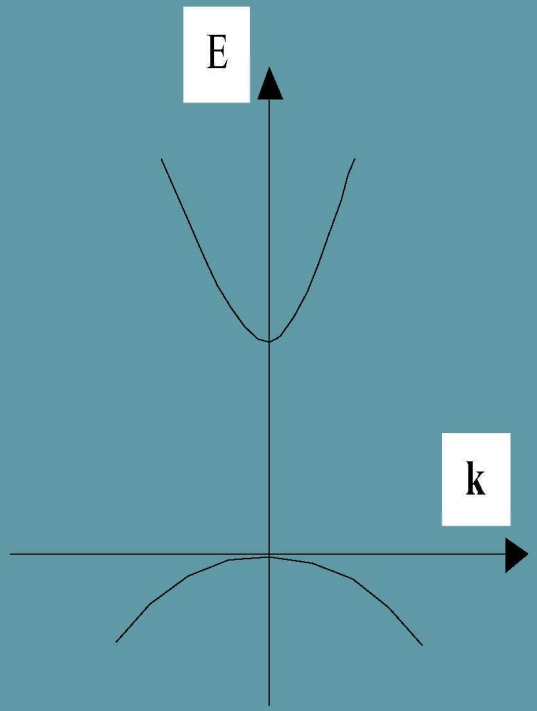

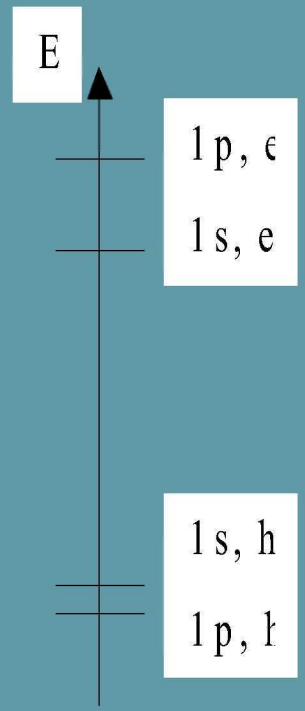

Bulk semiconductor **QD**

(e : electron, h : hole).

- Nanometer-size crystals of inorganic solids are the topic of much current research area in materials physics and chemistry.
- The physical properties of such crystals vary systematically as a function of size, according to scaling laws.
- Nanoscience attempts to make and organize materials on the 1-10 nm length scale, and also to understand the evolution of the bulk properties from the molecular properties in this region.
- Very small clusters are essentially molecules with chemical bonding different from that in the bulk.

As a cluster grows, it will at some size adopt the unit cell and bonding of the bulk lattice – Such particles are NANOCRYSTALS or QUANTUM DOTS (QDs).

Nanocrystals are crystalline matter that is very finely divided, but it is still large compared with the atomic limit!

- The emission from a nanocrystal comes at a very specific energy, depending on the size.
- Nanocrystals may be thought of as a new class of tunable dye molecules

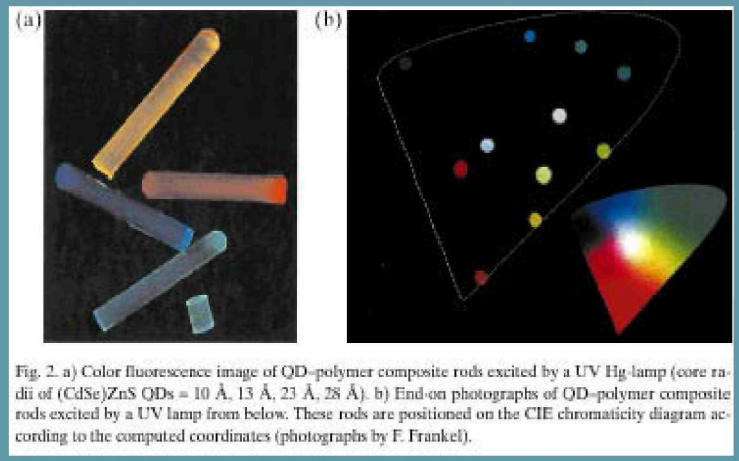

Fig. 2. a) Color fluorescence image of QD–polymer composite rods excited by a UV Hg-lamp (core radii of (CdSe)ZnS QDs = 10 Å, 13 Å, 23 Å, 28 Å). b) End-on photographs of QD–polymer composite rods excited by a UV lamp from below. These rods are positioned on the CIE chromaticity diagram according to the computed coordinates (photographs by F. Frankel).

Full Color Emission from II-VI Semiconductor Quantum Dot-Polymer Composites

By Jinwook Lee, Vikram C. Sundar, Jason R. Heine, Moungi G. Bawendi, and Klavs F. Jensen

A family of Qdot particles can be made to emit a full spectrum of colors when excited with a single excitation source.

The magnetron Rf-Sputtering technique has been applied to the fabrication of small crystal-size of: CdS-doped SiO2 films; CdS-doped Al2O3 films (Braga)

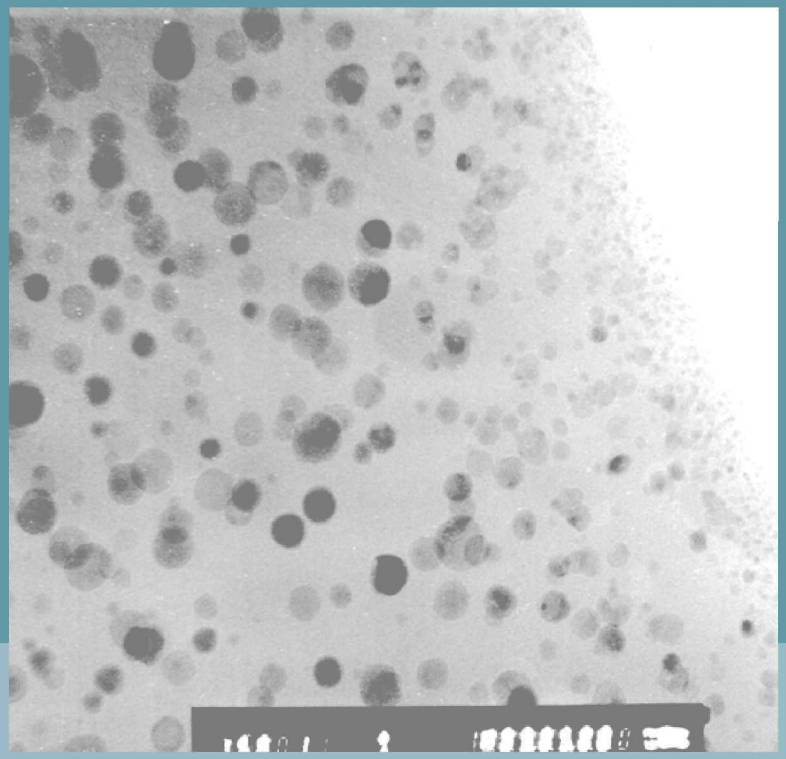

TEM image of CdS-annealed film (R#A8-3). The mean diameter is ~6nm.

Spherical Potentiel Well

$$\left(-\frac{\hbar^2}{2m^*}\nabla^2 + V_w(\vec{r})\right)F(\vec{r}) = E\,F(\vec{r})$$

$$V_w(\vec{r}) = \begin{cases} 0 & pour \quad r < R \\ V_0 & pour \quad r > R \end{cases} \qquad F_{n,l,m}(\vec{r}) = \phi_{n,l,m}(r)\,Y_l^m(\theta,\varphi)$$

$$-\frac{1}{r}\frac{d^2}{dr^2}\left(r\,\phi_{n,l,m}(r)\right) + \left(\frac{l(l+1)}{r^2} - k^2\right)\phi_{n,l,m}(r) = 0 \qquad r < R$$

$$-\frac{1}{r}\frac{d^2}{dr^2}\left(r\,\phi_{n,l,m}(r)\right) + \left(\frac{l(l+1)}{r^2} + \kappa^2\right)\phi_{n,l,m}(r) = 0 \qquad r > R$$

The solutions which are regular in the origin and at infinity are given by the spherical Bessel functions $j_l(kr)$ and $h_l(kr)$

$$V_0 \to \infty \qquad \phi_{n,l,m}(r) = \sqrt{\frac{2}{R^3}}\,\frac{j_l(kr)}{j_{l+1}(kR)} \qquad j_l(\alpha_{n,l}) = 0 \qquad k = \frac{\alpha_{n,l}}{R}$$

$$E_{n,l} = \frac{\hbar^2}{2m^*}\frac{\alpha_{n,l}}{R^2}$$

Optical Transitions in a QD

$$V_0 \to \infty$$

$$E_{e,nlm} = E_g + \frac{\hbar^2}{2m_e^*}\left(\frac{\alpha_{n,l}}{R}\right)^2$$

$$E_{h,nlm} = \frac{\hbar^2}{2m_h^*}\left(\frac{\alpha_{n,l}}{R}\right)^2$$

En absence d'interaction coulombienne, l'état de plus basse énergie de la paire électron-trou a une énergie plus grande que le gap du semiconducteur massif d'une quantité

$$\Delta E = \frac{\hbar^2}{2\mu}\left(\frac{\pi}{R}\right)^2 = E_{ex}\left(\frac{\pi a_B}{R}\right)^2$$

Dans les petits QD l'énergie nécessaire à la création d'une paire électron-trou est donnée par:

$$R \langle\langle a_B$$

$$\hbar\omega = E_g + E_{ex}\left(\frac{\alpha_{n,l} a_B}{R}\right)^2$$

CONFINED ELECTRONIC STATES IN SEMICONDUCTOR QDS

Semiconductors quantum dots (QDs) possess discrete excitonic and phonon spectra. For a spherical QD of radius *R*, the excitonic spectrum in the effective mass approximation (EMA) is well known [*Ekimov A.I. et al*, *JOSA (B)* (1993)]:

$$E(R) = E_g + \frac{\hbar^2 \alpha_e^2}{2m^*_e R^2} + \frac{\hbar^2 \alpha_h^2}{2m^*_h R^2} - 1.786 \frac{e^2}{\kappa R} - 0.248 E_{ex}$$

where E_g is the bulk band gap energy, R is the radius of the nanoparticle which assume to be spherical, α_e and α_h are the roots of a certain characteristic equation, e is the electron charge and ħ is the Plank´s constant, me* and mh* are the effective masses of the electron and hole, and and κ and E_{ex} are the relative dielectric constant and bulk exciton energy of the QD material.

- The systematic variation of the density of electronic states as a function of the size is seen clearly in the optical absorption spectra of semiconductors.
- In smaller nanocrystals, the threshold energy for absorption is shifted to higher energy (lower wavelength), and the spectra start to develop discrete features.

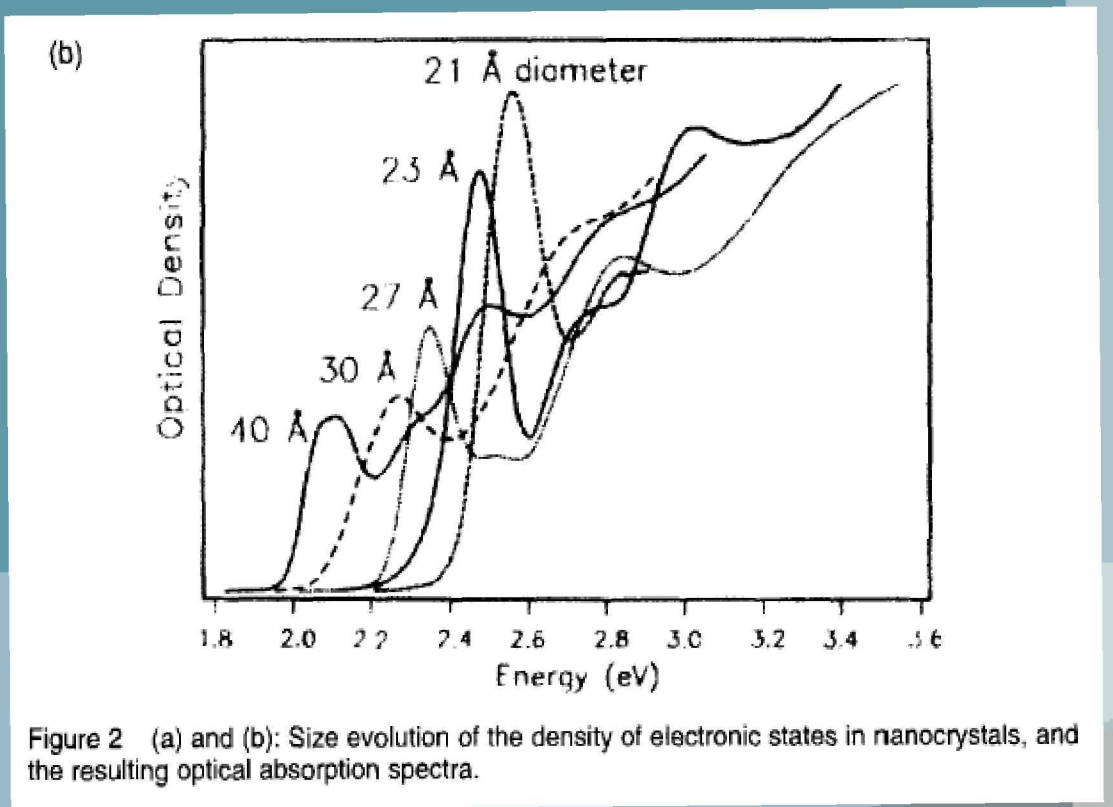

Figure 2 (a) and (b): Size evolution of the density of electronic states in nanocrystals, and the resulting optical absorption spectra.

OPTICAL EXCITATION

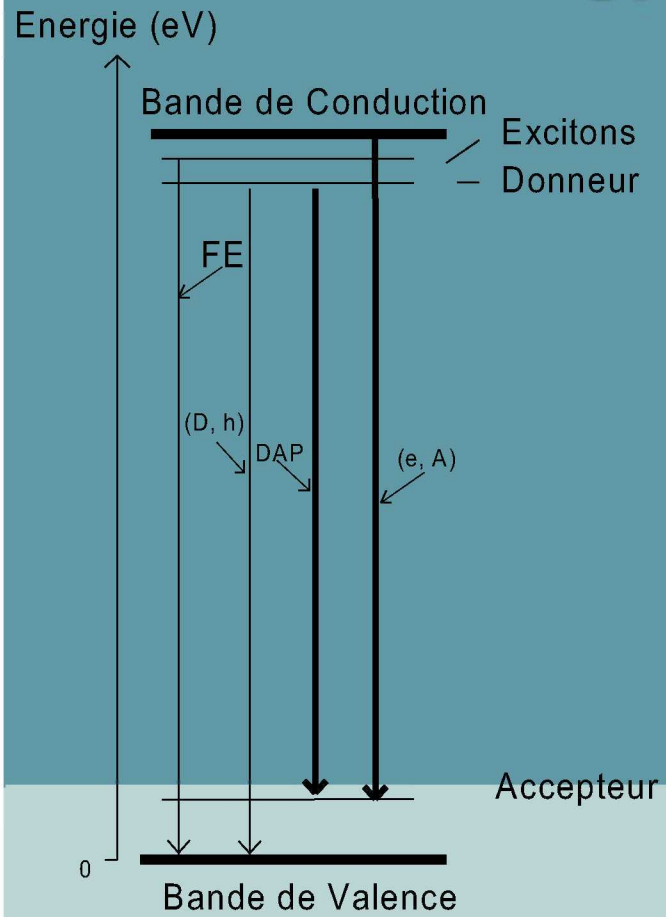

- Exciton: bound electron-hole pair (EHP)

Excite semiconductor → creation of EHP

- There is an attractive potential between electron and hole

mh* > me* ⇒ hydrogenic system

Binding energy determined from Bohr Theory

In QDs, excitons generated inside the dot

- The excitons confined to the dot

– Degree of confinement determined by dot size

– Discrete energies

Optical Transitions

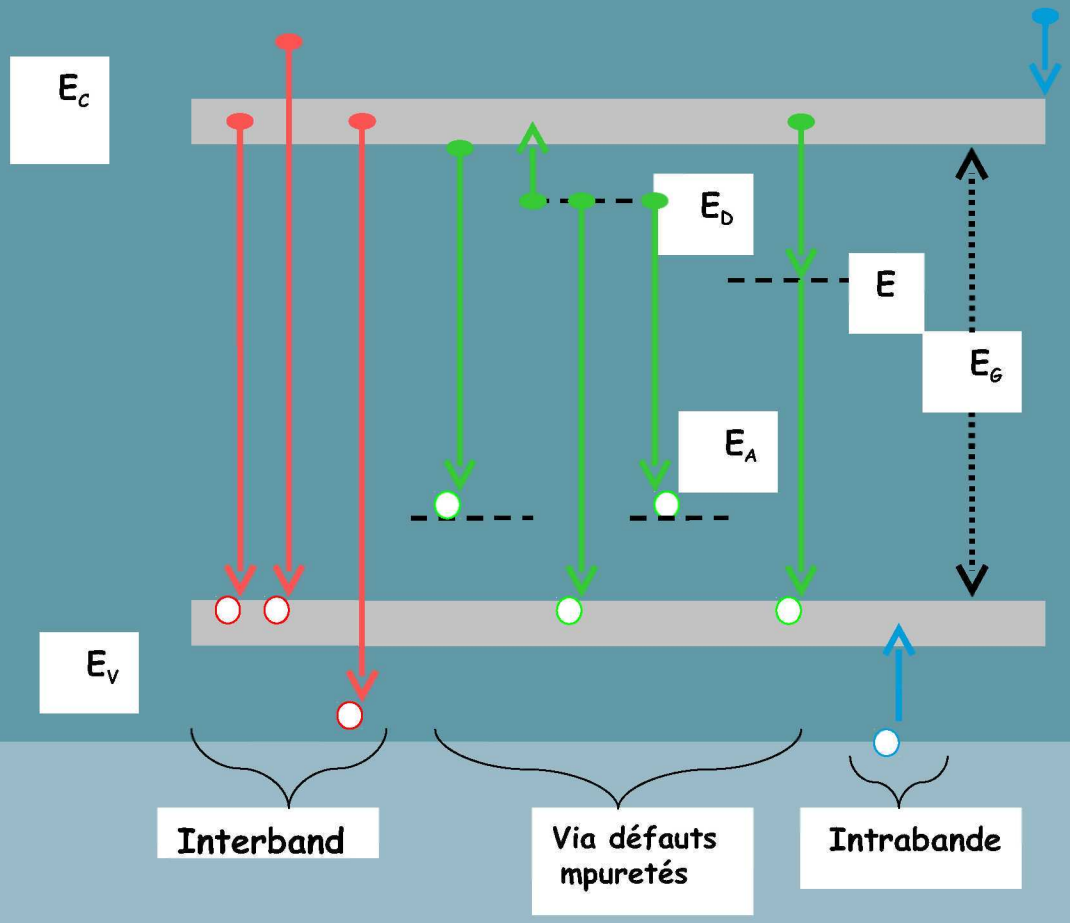

Les trois principales transitions optiques au sein d'un semiconducteur

Transition bande à bande (sc à gap direct)

- Le coefficient d'absorption est donné par:

$$\alpha(h\nu) = A^*\left(h\nu - E_g\right)^{1/2} \qquad A^* \approx \frac{q^2(2m_r)^{3/2}}{nch^2 m_e^*}$$

- Pour une bande parabolique, on a:

$$E_f - E_g = \frac{\hbar^2 k^2}{2m_e^*} \qquad E_i = \frac{\hbar^2 k^2}{2m_h^*}$$

$$h\nu - E_g = \frac{\hbar^2 k^2}{2}\left(\frac{1}{m_e^*} - \frac{1}{m_h^*}\right)$$

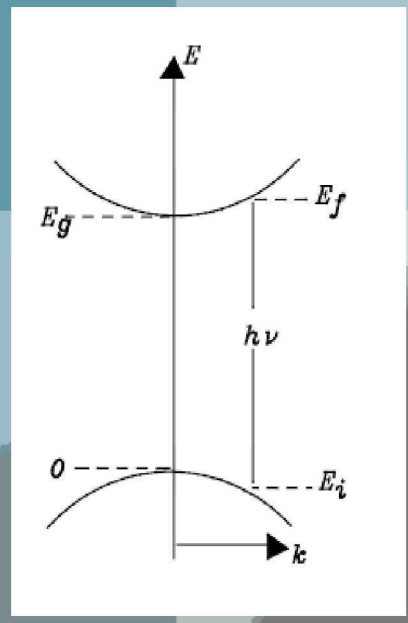

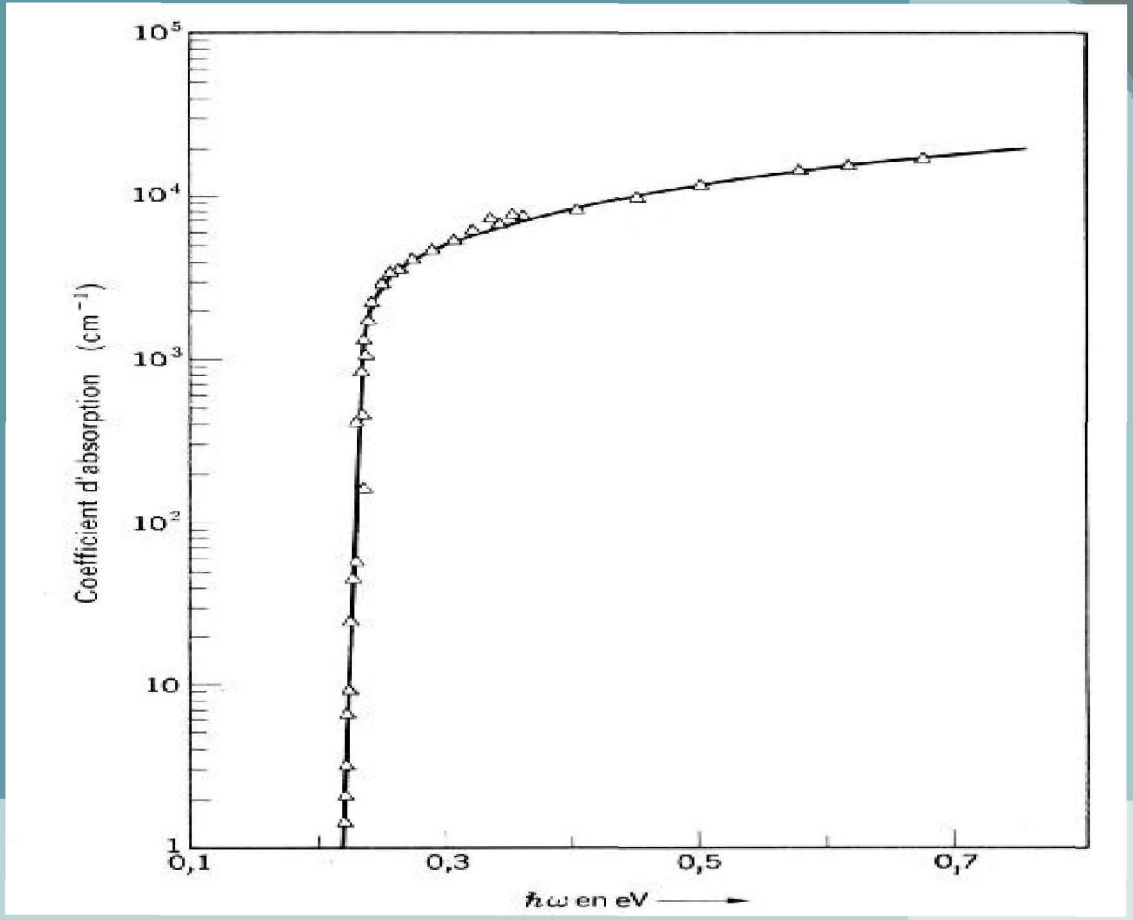

absorption optique dans l'antimoniure d'indium pur (InSb) qui est un semiconducteur à gap direct

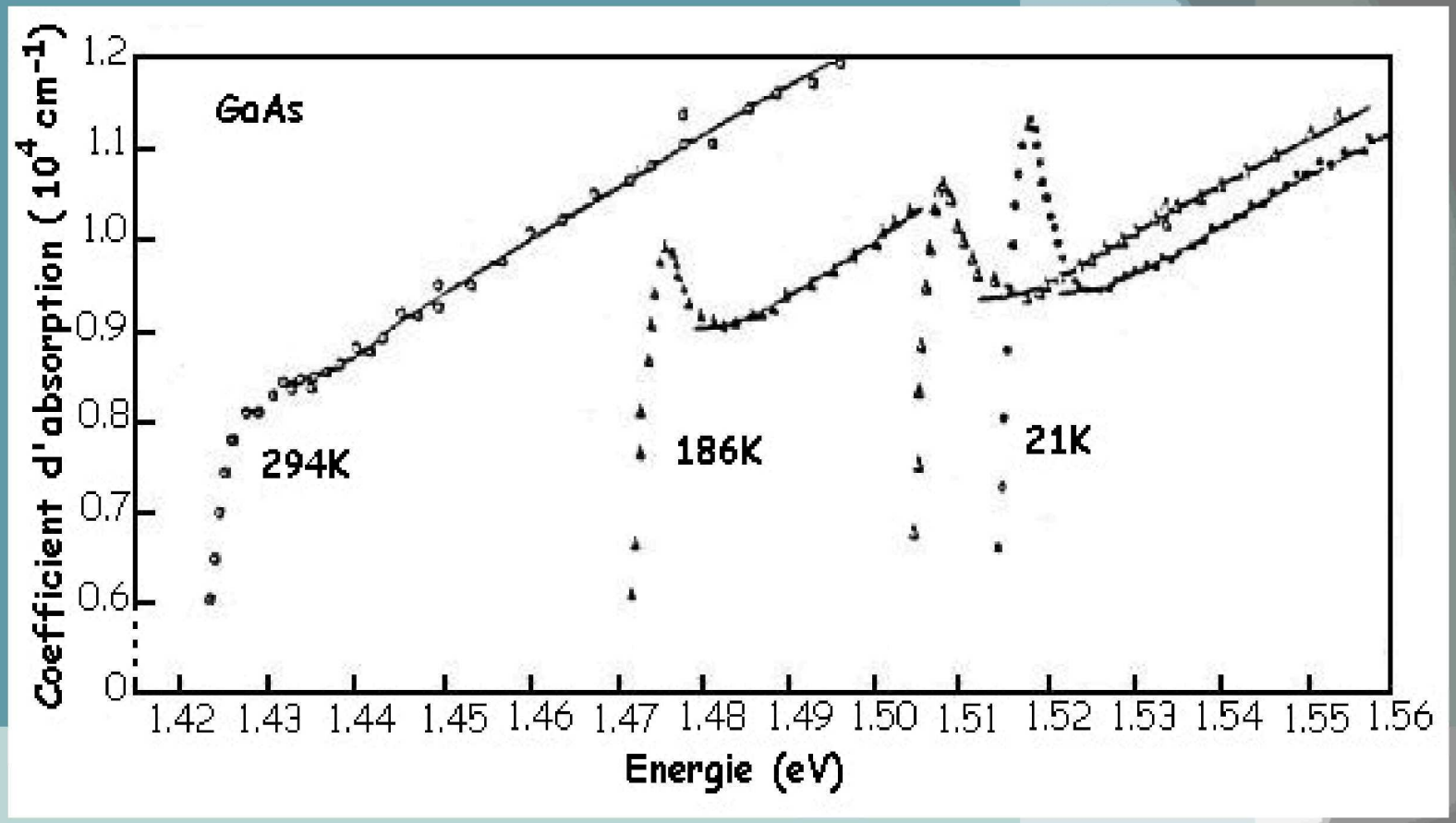

Absorption par exciton dans le cas du semiconducteur à gap directe gaas. on observe un pic très prononcé qui s'élargit lorsque la température est augmentée.

Absorption coefficient of magneto-donor in a Quantum Dots

$$\alpha(\omega) = \frac{\pi e^2}{n_r c \varepsilon_0 m^{*2} \omega V} \sum_{i,f} \left| \langle f | H_{int} | i \rangle \right|^2 \delta(E_f - E_i - \omega)$$

with

$$H_{int} = \varepsilon . \left(p + \frac{e}{c} A \right)$$

$|i\rangle$ is the initial state of the donor (occupied) and E_i is its corresponding energy

$|f\rangle$ is the final sate (empty) and E_f is its corresponding energy

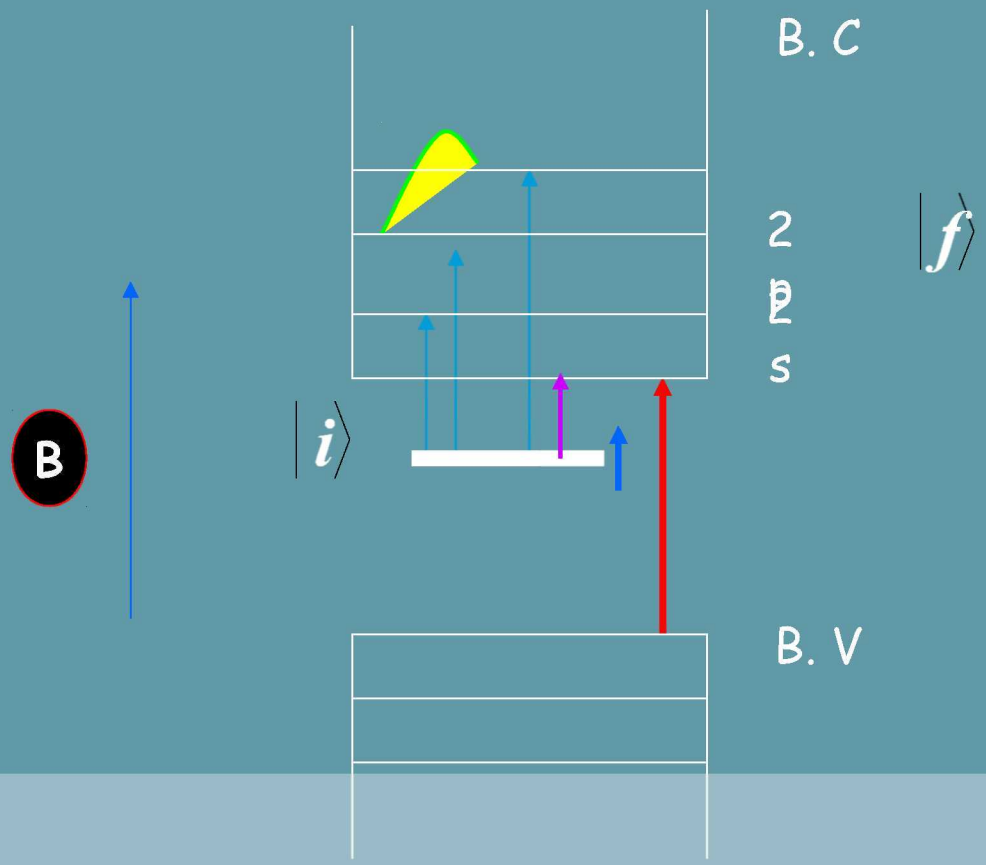
B. C
2
p
s
$|f\rangle$
B
$|i\rangle$
B. V

$$H\,\psi_i(x,y,z) = E(\eta)\,\psi_i(x,y,z)$$

$$H = T + V + W + M + V_w(x,y,z)$$

Kinetic Energy: $T = -\Delta$ $\qquad R^* = \dfrac{m^* e^4}{2\varepsilon^2 \hbar^2}$

Coulomb Energy $V = -\dfrac{2}{r}$ $\qquad a^* = \dfrac{\varepsilon \hbar^2}{e^2 m^*}$

Electric Energy $W = \eta . z$ $\qquad \eta = \dfrac{e a^* F}{R^*}$

Magnetic Energy $M = \dfrac{\gamma^2}{4}\left(x^2 + y^2\right) + \gamma L_z$ $\qquad \gamma = \dfrac{\hbar eB}{2R^* m^* c}$

→ Niveaux de Landau : e^- de la B.C (pas de forme Coulombienne)

$$H_o \rightarrow \frac{\hbar^2}{2m^*}\left(-i\nabla + \frac{e}{\hbar c}\vec{A}_o\right)^2 + \frac{1}{2}g_o\mu_B\vec{B}_o\cdot\vec{\sigma}$$

$$\vec{B}_o = \nabla \times \vec{A}_o, \qquad \vec{B}_o = B_o(0,0,1)$$

$$E_n(k_\zeta) = \frac{\hbar e B_o}{m^* c}\left(n+\frac{1}{2}\right) + \frac{1}{2}g_o\mu_B B_o(\pm 1) + \frac{\hbar^2 k_\zeta^2}{2m^*}$$

$$n = 0, 1, 2, \ldots..$$

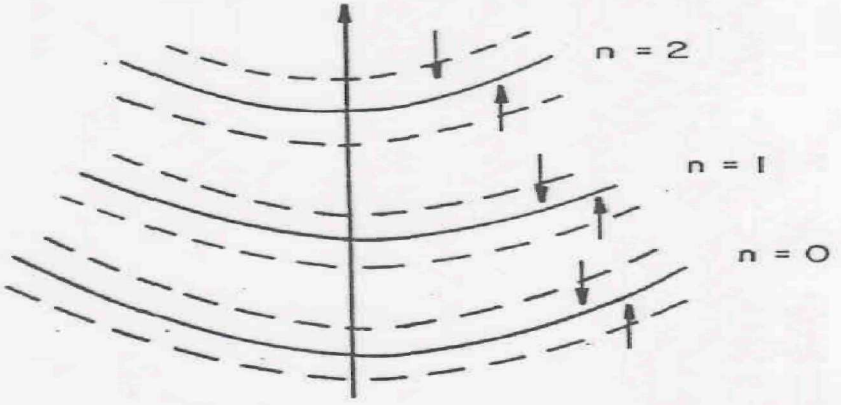

Pour le niveau de Landau de plus basse énergie ($n=0$, $k_\zeta = 0$) la fonction d'onde est donnée par:

$$|\psi_0\rangle = \sqrt{\frac{\gamma}{2\pi}}\, e^{-\frac{\gamma}{4}(x^2+y^2)}$$

résultat obtenu également à partir de la fct d'onde de Y.K.A en passant à la limite:

$$\begin{cases} a_t = 1/\sqrt{8} \\ a_l = a \quad (\text{i.e. } \xi = \frac{a}{a^*} = 0) \end{cases}$$

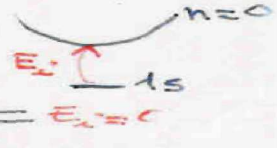

Comportement dans un champ magnétique

$(\hat{\xi}, \hat{\eta}, \hat{\zeta})$ $\quad \vec{B}_0 \parallel \hat{\zeta}$

$$H_0 = -\nabla^2 - \frac{2}{r} + \gamma L_\zeta + \frac{1}{4}\gamma^2(\xi^2+\eta^2)$$

$$\gamma = \frac{\hbar\omega_c}{2R^*} = \mu_B \frac{m_0}{m^*}\frac{B_0}{R^*}$$

- énergie : $R^* = \frac{m^* e^4}{2\varepsilon_\infty^2 \hbar^2}$
- longueur : $a^* = \frac{\varepsilon_\infty \hbar^2}{m^* e^2}$

$\{ B_0$ Labo.
$\{ m^*, \varepsilon_\infty$ (S.C.)

$\gamma \ll 1$: b) $\gamma \geq 1$

$\gamma = 0$: Atome d'hydrogène $\quad \varphi_{sph}(r) = \frac{1}{\sqrt{\pi a^3}} e^{-r/a}$

$$\boxed{\gamma \propto \frac{B_0 \varepsilon_\infty^2}{m^{*2}}}$$

$\gamma \gg 1$: Les niveaux de Landau (en absence du potentiel Coulombien : e^- de la B.C.)

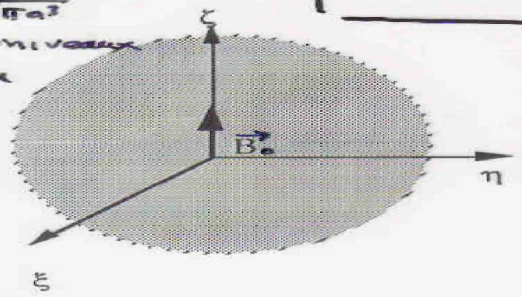

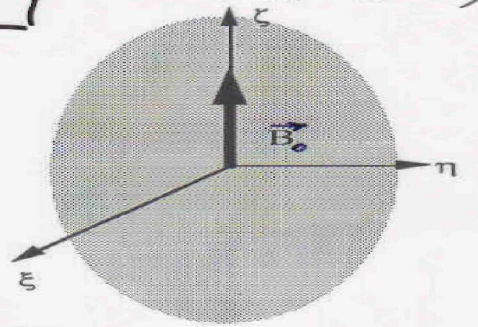

InSb : $B_0 = 10\,T$, $m^* = 0.01\, m_0$ $\longrightarrow$ $\gamma \simeq 80$

a_t et a_ℓ sont des paramètres variationnels

$$|0\rangle = \frac{1}{\sqrt{2^{\frac{3}{2}}\pi^{\frac{3}{2}} a_t^2 a_\ell}} \exp -\left[\frac{\xi^2+\eta^2}{4a_t^2} + \frac{\zeta^2}{4a_\ell^2}\right]$$

Fonction d'onde de Y.K.A (1956)
Fct d'onde type oscillateur

Relations de passage au niveau de Landau de plus basse énergie

$$a_t = \frac{1}{\sqrt{\gamma}}$$

$$a_\ell = \infty \quad \left(\text{c.à.d. } \varepsilon = \frac{a_t}{a_\ell} = 0\right)$$

$$|n=0\rangle = \sqrt{\frac{\gamma}{2\pi}}\, e^{-\frac{\gamma}{4}(\xi^2+\eta^2)}$$

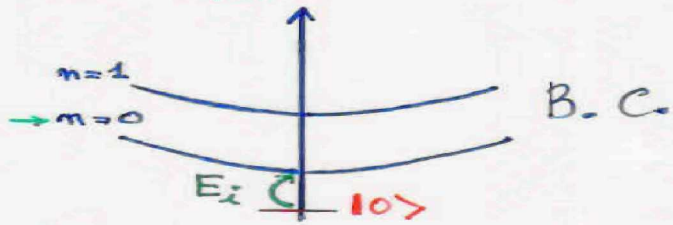

γ	col. 1		col. 2			col. 3			Col. 4	Col. 5	Col. 6	Col. 7	Col.
	E	a	E	a_t	a_l	E	a_t	a_l	E	E	E	E	E
0.1	-.995	.9[illegible]	-.995	.995	.997	-.844	.934	.936		-.995	-.995	-.995	
0.2	-.980	.981	-.980	.978	.988					-.981	-.981	-.981	
0.3	-.957	.9[illegible]2	-.957	.958	.976					-.958	-.957	-.958	
0.4	-.925	.938	-.926	.928	.960					-.929	-.925	-.929	
0.5	-.887	.931	-.888	.901	.945	-.750	.844	.887		-.894	-.841	-.894	
0.6	-.842	.888	-.845	.874	.929					-.853	-.835	-.855	
0.7	-.792	.863	-.797	.847	.912					-.810	-.787	-.814	
0.8	-.738	.841	-.744	.823	.900					-.762	-.710	-.765	
0.9	-.650	.818	-.689	.800	.855					-.712	-.634	-.715	
1	-.617	.798	-.629	.778	.873	-.524	.728	.820	-.661	-.659	-.551	-.662	-.364
2	.135	.648	.076	.624	.777	.092	.583	.727		-.035		-.044	
3	1.028	.559	.901	.536	.717	.809	.499	.671		0.686		0.671	
4	2.000	.487	1.787	.477	.675	1.580	.444	.631		1.459		1.438	
5	3.022	.456	2.713	.435	.645	2.385	.357	.614	2.25	2.265		2.239	
10	8.548	.339	7.650	.319	.561	6.669	.297	.516					6.659
20	20.495	.248	18.143	.231	.472	15.769	.215	.441					15.694
25	26.681	.223	23.526	.208	.449	20.435	.193	.419	20.627				
30	32.951	.205	28.952	.191	.431	25.145	.177	.403					25.024
40	45.669	.179	39.232	.166	.404	34.656	.155	.385					34.496
50	58.558	.161	50.999	.147	.384	44.245	.139	.359					44.053
60	84.665	.147	62.131	.136	.369	53.891	.127	.341					53.669
70	84.665	.137	73.311	.126	.356	63.595	.116	.341					63.329
75	91.242	.133	78.715	.122	.352	68.432	.228	.658					
80	97.836	.128	84.027	.118	.347	73.294	.110	.325					73.021
90	111.066	.121	95.772	.112	.338	83.037	.104	.316					82.740
100	124.346	.115	107.041	.106	.330	92.800	.099	.309	92.543				92.480

$\frac{1}{\sqrt{\pi a^3}} e^{-r/a}$ Sph.

$A \exp-\left[\frac{\xi^2+\eta^2}{a_t^2} + \frac{\rho^2}{a_l^2}\right]^{1/2}$ cylind.

$A \exp-\left[\frac{\xi^2+\eta^2}{4a_t^2} + \frac{\rho^2}{4a_l^2}\right]$ Y.K.A.

" modèle à 4 paramètres " Laser

sym. cylind

Combin. CABIB

NUM. Repris

NUM.

fct d'onde de DEXTER : $A \exp-\left[\frac{\xi^2+\eta^2}{a_t^2} + \frac{\rho^2}{a_l^2}\right]^{1/2\lambda}$ (3 paran.).

Col. 1 = Fonction sphérique 2.58.
Col. 2 = Fonction hydrog. cylindrique 2.62
Col. 3 = Fonction de Yafet et al.[23] 2.65.

Col. 4 = Résultats de Larsen.[26]
Col. 5 = Résultats de Pokatilov-Rusanov.[25]
Col. 6 = Résultats de Brandi.[27]
Col. 7 = Résultats de Cabib-Fabri-Fiorio.[28]
Col. 8 = Résultats de Rodrigues

Initial state

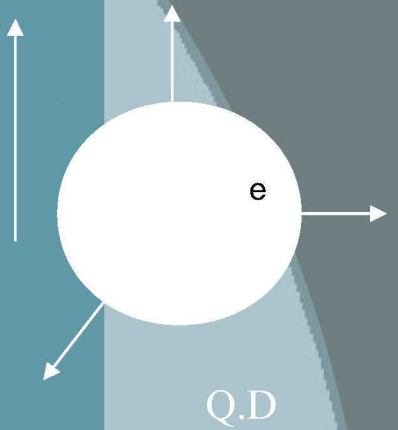

$$H = -\Delta - \frac{2}{r} + \gamma L_z + \frac{1}{4}\gamma^2 r^2 \sin^2(\theta) + V(\vec{r})$$

$$V(r) = \begin{cases} 0 & r \le R \\ \infty & r > R \end{cases} \qquad \gamma = \frac{e\,B}{2m^* c R_B^*} \qquad a_B^* = \frac{\varepsilon_0}{m^* e^2} \qquad R_B^* = \frac{e^2}{2\varepsilon_0 a_B^*}$$

crystals	$a_B^*(A^\circ)$	$R_B^*(meV)$	γ
CuCl	6.896	192.840	0.0145
CuBr	11.910	115.500	0.0431
CdS	24.981	33.882	0.190
CdSe	39.878	18.406	0.484
ZnS	9.824	140.831	0.029

Values of the effective units of length, energy and magnetic field for B=20T.

eigenfuction

$$\psi(r,\theta,\varphi)=\begin{cases} N_0(\lambda)\dfrac{J_{1/2}(k_{10}r)}{\sqrt{r}}exp(-\lambda r)exp\left(-\dfrac{1}{4}\gamma r^2 sin^2(\theta)\right) & r<R \\ 0, & r\geq R \end{cases}$$

boundary condition

$$\psi(r=R,\theta,\varphi)=0$$

eigenvalue

$$E_\lambda=\frac{\langle\psi|H|\psi\rangle}{\langle\psi|\psi\rangle}$$

final state

$$H = -\Delta + \gamma L_z + \frac{1}{4}\gamma^2 r^2 \sin^2(\theta) + V(\vec{r})$$

$$H = H_0 + H'$$

$$H_0 = -\Delta + \gamma L_z + V(r)$$

$$H' = \frac{1}{4}\gamma^2 r^2 \sin^2(\theta)$$

$$H_0 \, \Phi_{n\ell m}(r) = E^0_{n\ell m} \, \Phi_{n\ell m}(r)$$

we use the second ordre perturbation theory

$$\Phi_{n\ell m}(r) = N_{n\ell}\, Y_{\ell}^{m}(\theta,\varphi)\, \frac{J_{\ell+1/2}(k_{\ell n} r)}{\sqrt{r}}$$

$$E_{n\ell m} = E^{0}_{n\ell m} + \frac{1}{4}\gamma^{2} N^{2}_{n\ell} \Lambda_{n\ell} \left(1 - \frac{(\ell+m+1)(\ell-m+1)}{(2\ell+1)(2\ell+3)} - \frac{(\ell+m)(\ell-m)}{(2\ell+1)(2\ell-1)} \right)$$

$$\Lambda_{n\ell} = R^{4} \int_{0}^{1} t^{3}\, J^{2}_{\ell+1/2}(k_{n\ell} R\, t)\, dt$$

$$E^{0}_{nlm} = k^{2}_{n\ell} + m\gamma$$

$$-\ell \le m \le +\ell$$

The quantities $k_{n\ell}$ are given as solutions of the following equation

$$J_{\ell+1/2}(k_{\ell n} R) = 0$$

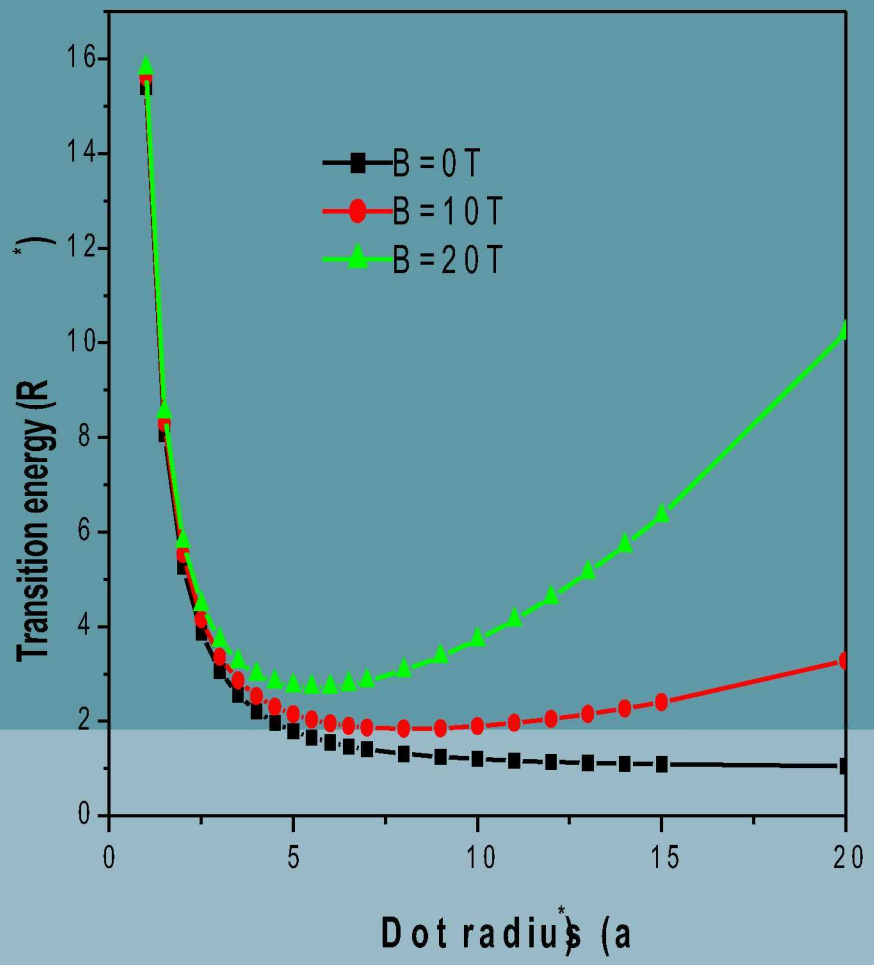

The 1s-2p+ transition energy as function of a dot radius for a magnetic field from 0 to 20T.

- $R < a^*$ and $\gamma < 1/R^2 \Rightarrow$ Et ~ % B
- $\gamma = 1/R^2 \Rightarrow$ Et
- $R >> a^*$ and $\gamma > 1/R^2 \Rightarrow$ Et ↗

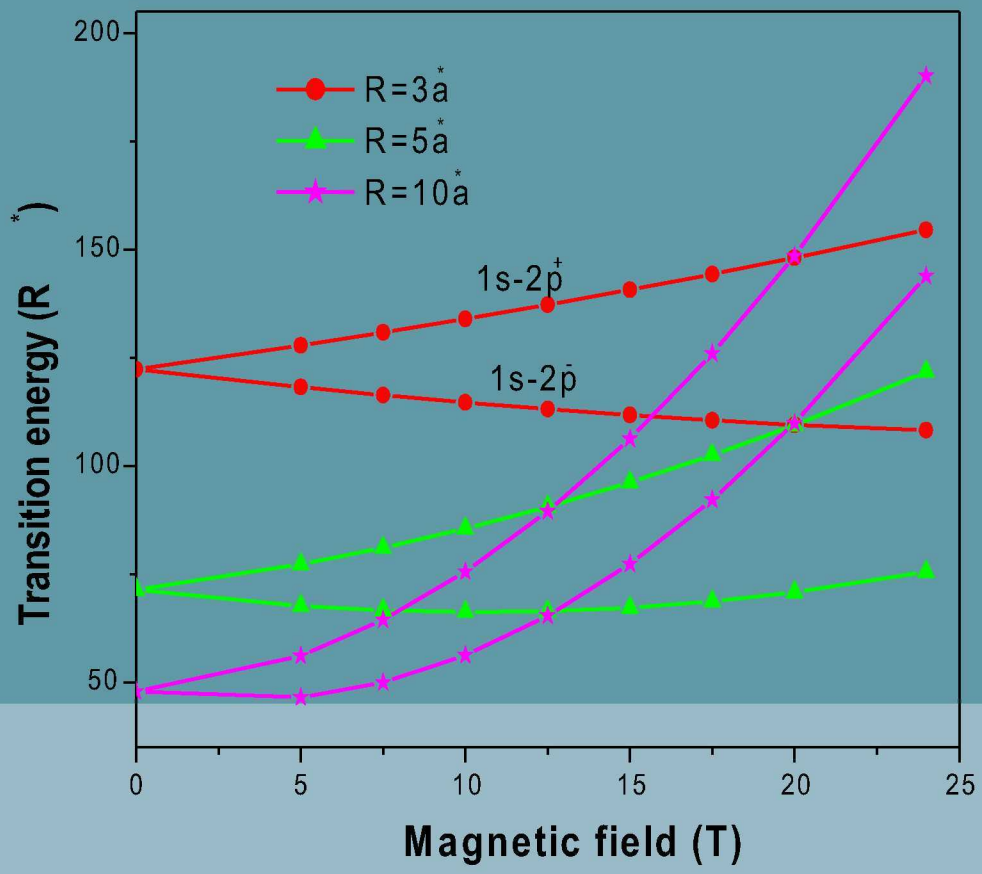

- $E_{1s\text{-}2p+}$ $\nearrow$ $\forall\ \gamma$ and R
- $E_{1s\text{-}2p-}$ $\nearrow$ if $\gamma > 1/R^2$
- $E_{1s\text{-}2p-}$ $\searrow$ if $\gamma < 1/R^2$

The 1s-2p+ transition energy and the 1s-2p- transition energy as function of the magnetic field

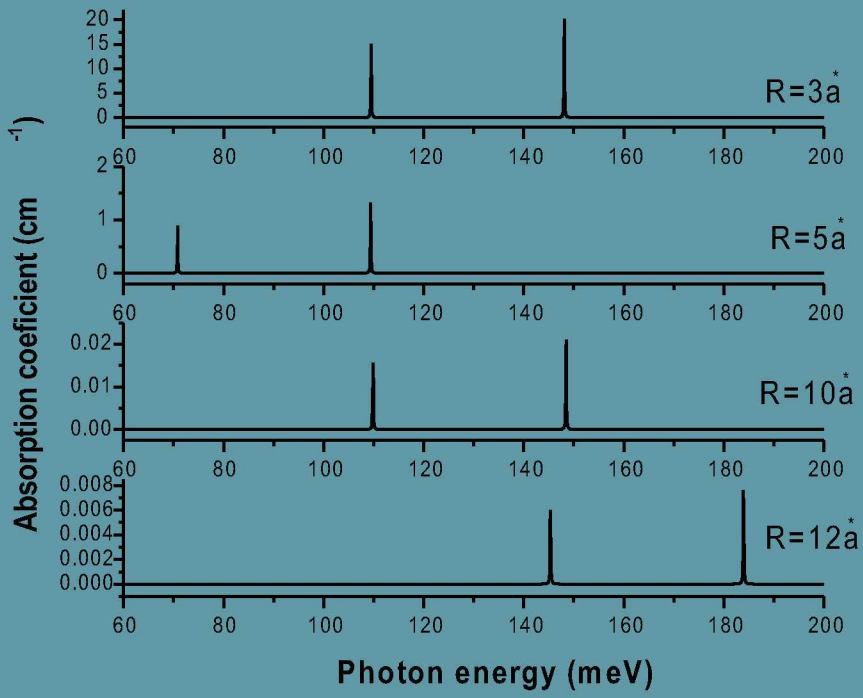

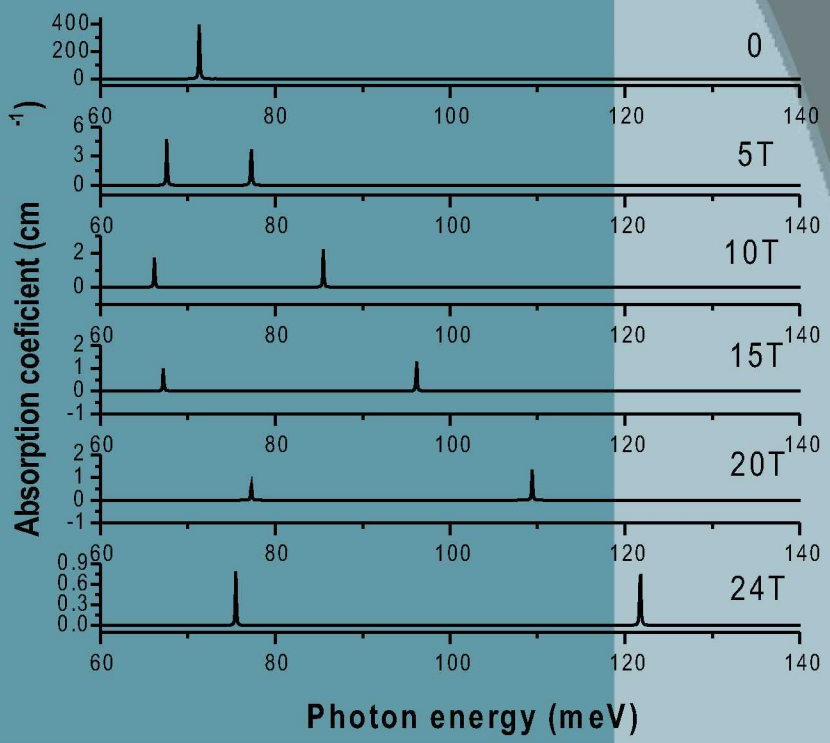

The application of the magnetic field induced reduction of the absorption peak and a displacement of the threshold energy.

Threshold ↘ if $\gamma < 1/R^2$

Threshold ↗ if $\gamma > 1/R^2$

The Impurity position effect

$$\varphi(r,\theta,\varphi)=\begin{cases}\mathrm{N}(r_0,\lambda)\dfrac{J_{1/2}(k_{10}r)}{\sqrt{r}}\exp\left(-\lambda\sqrt{r^2+r_i^2-2rr_i\cos(\theta)}\right)\exp\left(-\dfrac{1}{4}\gamma r^2\sin^2(\theta)\right), & r\le R\\ 0, & r>R\end{cases}$$

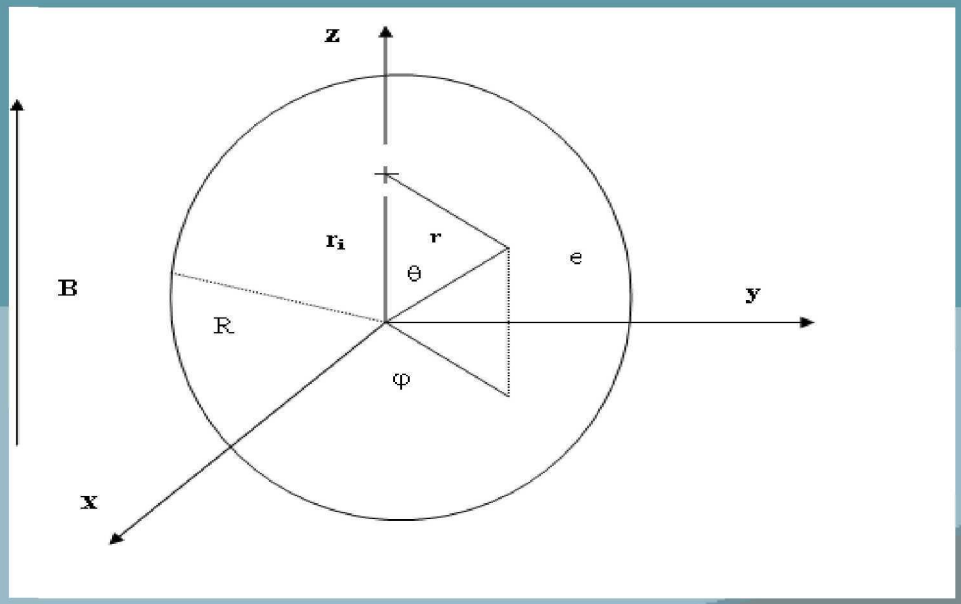

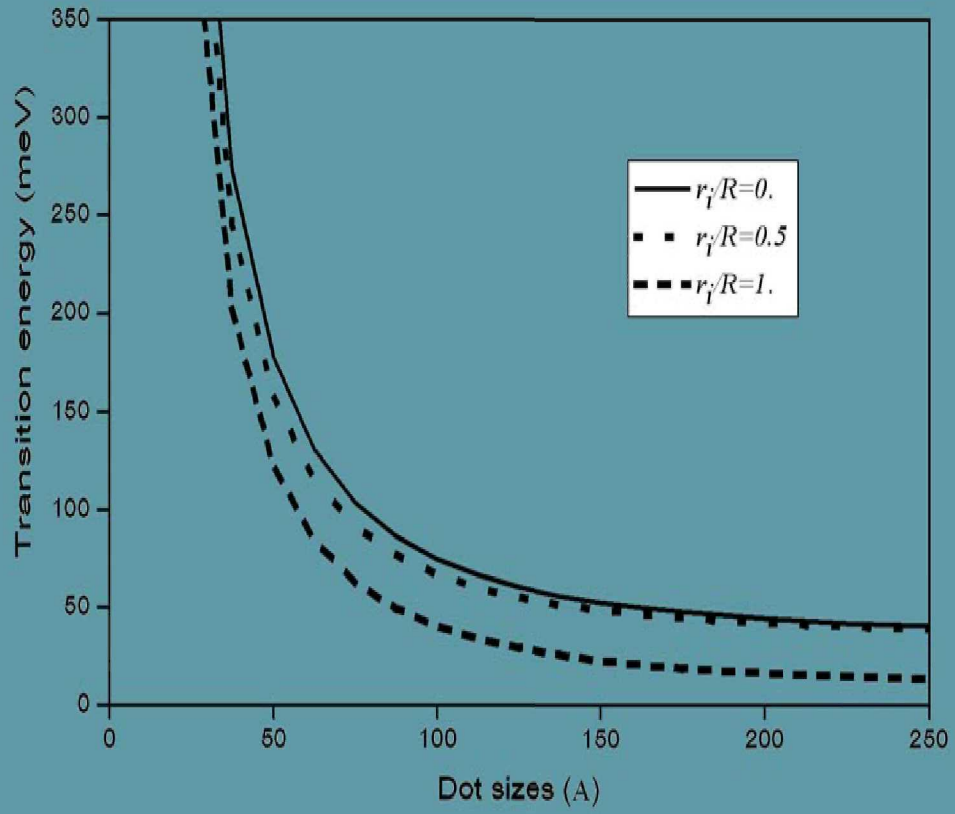

The 1s-2p transition energies as a function of the dot radii for different positions of the donor inside the CdS QD.

$$r_i/R = 0 \qquad r_i/R = 0.5 \quad r_i/R = 1$$

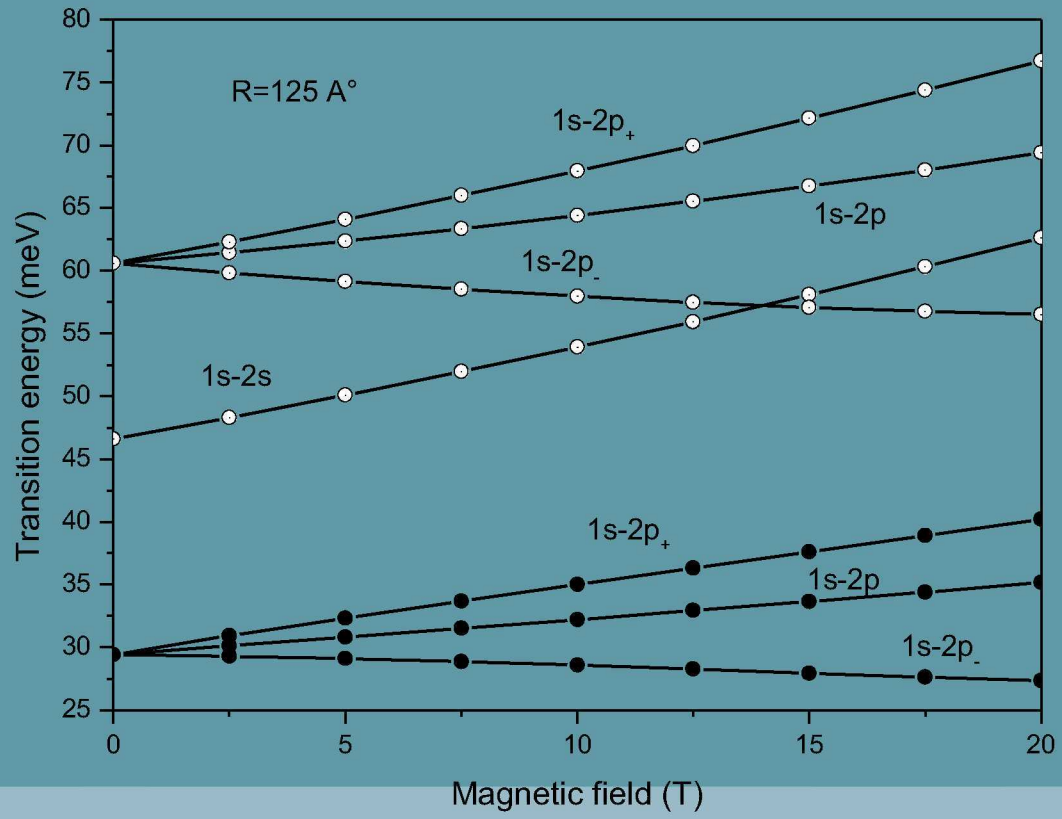

- **The transition energies between as a function of the magnetic field, for an on-center donor (open circles) and for an off-center donor (full circles).**

CdS

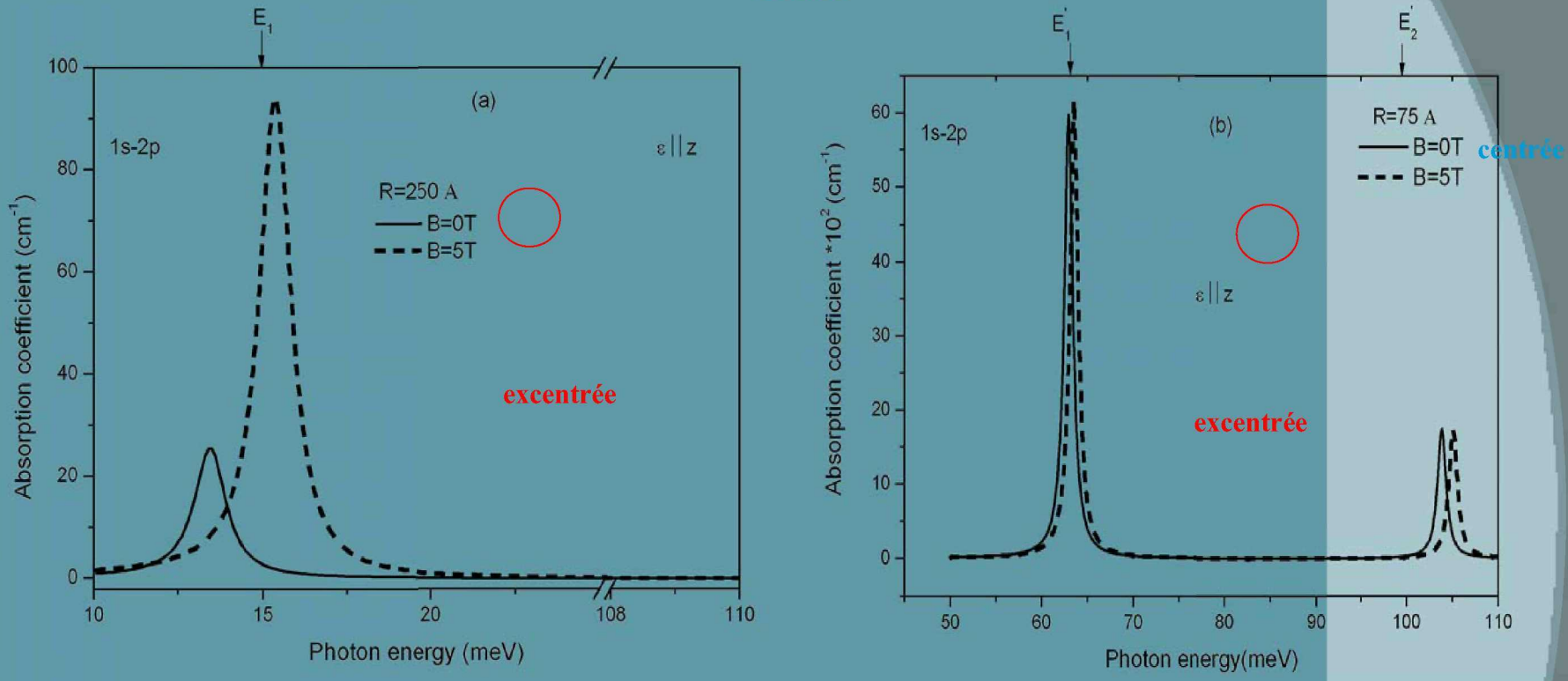

The peak value of the absorption coefficient for infinite CdS QD as a function of the photon energy for two magnetic field values B=0T and B=5T when the electromagnetic field is polarized parallel to r_i a) for a weak geometric confinement regime and b) for a strong geometric confinement regime. E1 and E2 correspond to transitions involving donor at the edge and at on-center of the QD respectively.

- The donor-related absorption spectra presents essentially two peaks; one at higher energy associated with impurities located at the QD center, and another at lower energies corresponding to transitions involving donors at the QD edge.
- The off center absorption peak is much larger
- For large QD there is only one peak at low energy associated with off center donor.

Polarisability of magneto-donor in a Quantum Dots

Magnetocapacitance measurement at low frequency (Low temperatures)

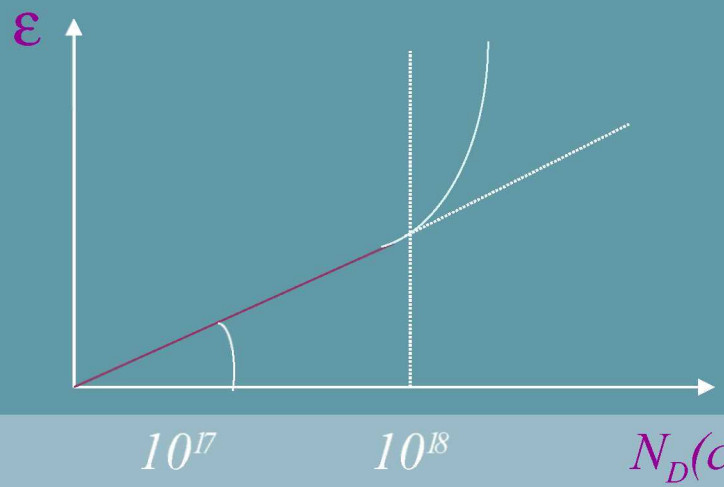

$$\frac{\varepsilon - 1}{\varepsilon + 2} = \frac{\alpha_p}{3} N_D$$

Clausius Mossoti

Cristal	Si			Ge
Impurity	Sb	P	As	Sb
α_{pxp} (10^5 Å^3)	3.1±0.3	2.4±0.4	1.0±0.1	68±15

- Perturbation:

$$E(\eta) = E(0) - 1/2\alpha_p F^2 \quad \Rightarrow \quad \alpha_p = \lim_{\eta \to 0} \frac{E(\eta) - E(0)}{F^2}$$

- Dipole moment :

$$\alpha_p = \frac{P}{F}$$

$$\Rightarrow \quad \alpha = \frac{\langle -e\,z \rangle_{\eta \neq 0} - \langle -e\,z \rangle_{\eta = 0}}{F}$$

CYLINDRICAL QUANTUM DOT

$$H = -\nabla^2 - \frac{2}{\sqrt{\rho^2 + z^2}} + \eta z + \frac{\gamma^2}{4}\rho^2 + \gamma L_z + V_w(\vec{r})$$

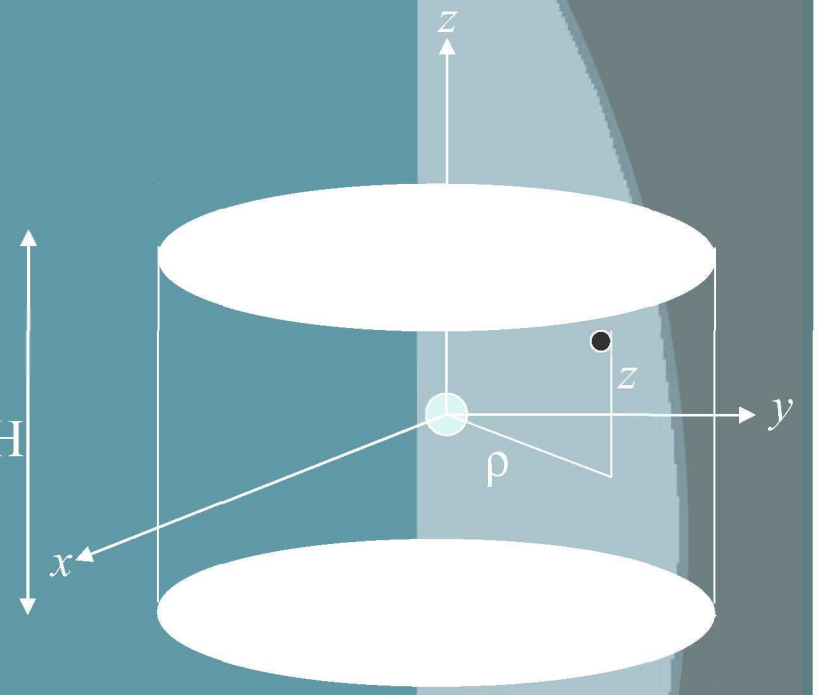

$$V_w(\rho,z) = \begin{cases} 0 & pour \quad \rho \langle R \; et \; |z| \langle H/2 \\ V_0 & pour \quad \rho \rangle R \; et \; |z| \langle H/2 \\ V_0 & pour \quad |z| \rangle H/2 \end{cases}$$

$$\psi_i(r) = \psi_0(\rho, z)(1 + \beta z)$$

Infinite potential

$$\psi_0(\rho, z) = NJ_0\left(\theta_0 \frac{\rho}{R}\right)\cos\left(\pi \frac{z}{H}\right)\exp\left(-\left(\frac{\rho^2}{8b^2} + \frac{z^2}{8a^2}\right)\right)$$

Finite potential

$$\psi_0(\rho, z) = N\phi(\rho)\phi(z)\exp\left(-\left(\frac{\rho^2}{8b^2} + \frac{z^2}{8a^2}\right)\right)$$

$$\phi(\rho) = \begin{cases} J_0(k_{1\rho}\rho) & pour \quad \rho < R \\ A_\rho K_0(k_{2\rho}\rho) & pour \quad \rho > R \end{cases}$$

$$\phi(z) = \begin{cases} \cos(k_{1z}z) & pour \quad |z| < \frac{H}{2} \\ A_z \exp(-k_{2z}|z|) & pour \quad |z| > \frac{H}{2} \end{cases}$$

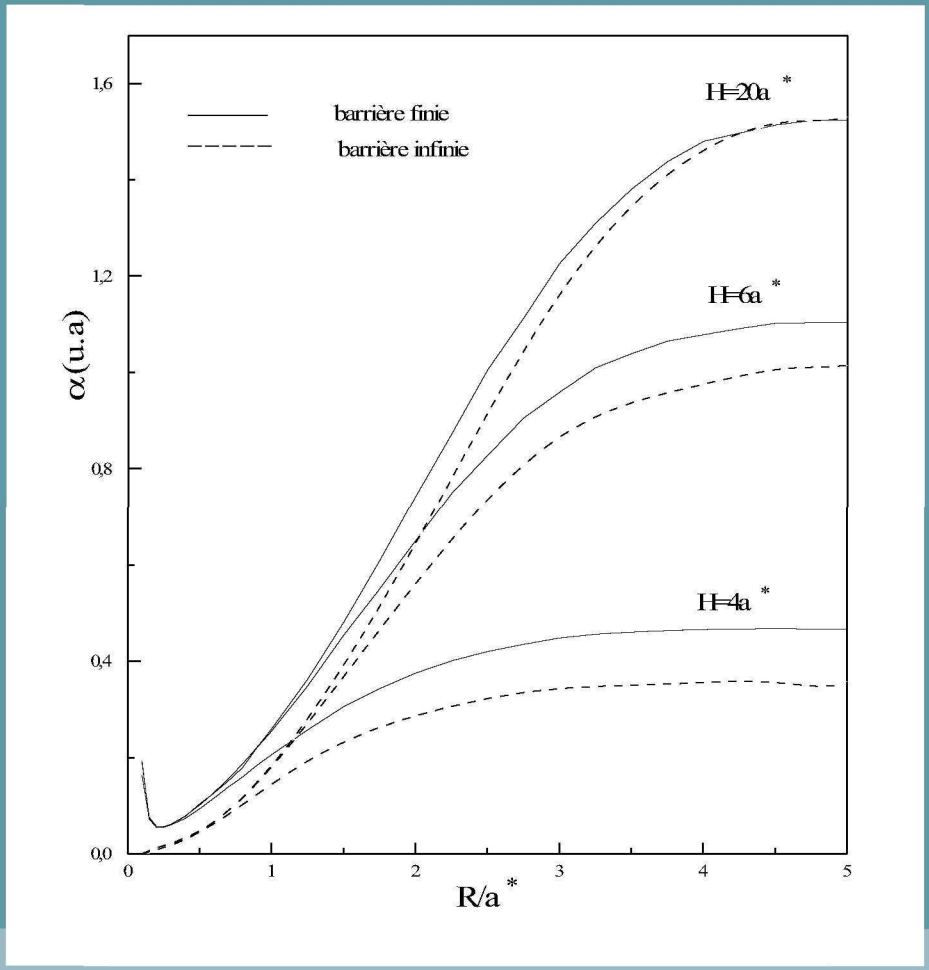

The polarizability values as a function of the dot radius and several values of length (finite and infinite barrier).

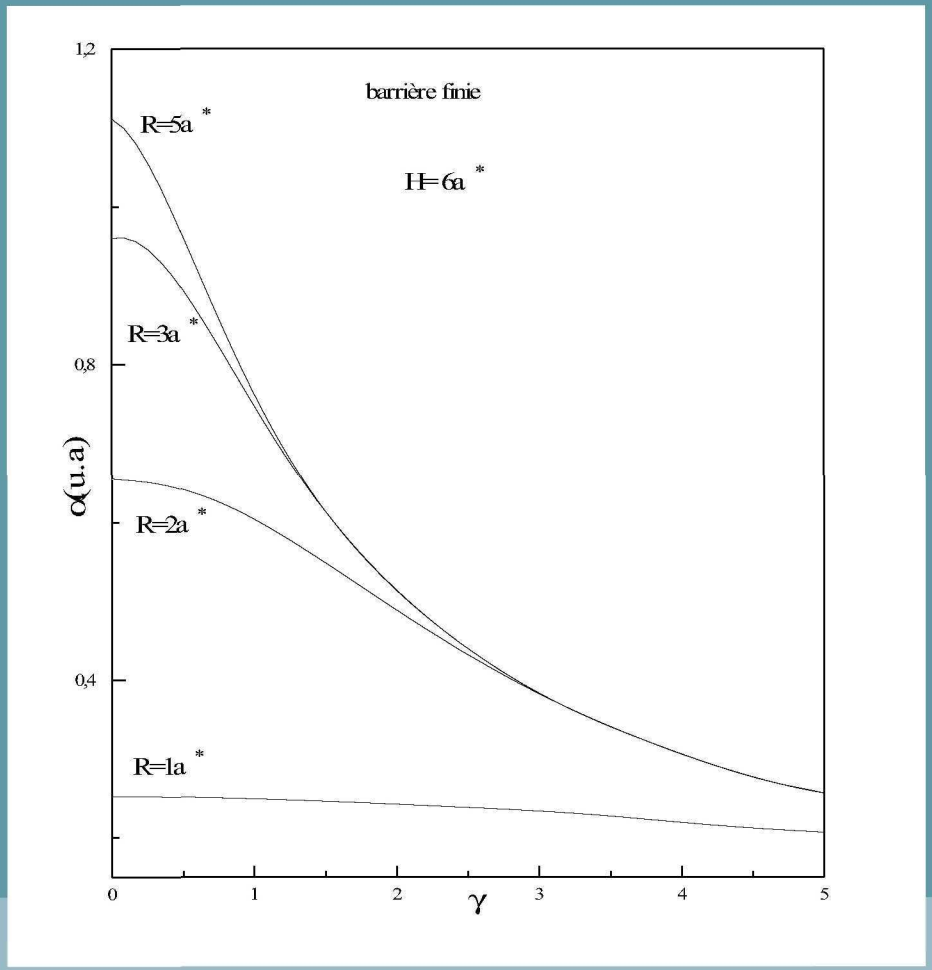

The polarizability as a function of the magnetic field intensity γ for several values of the radius R and for the length H=6a*(finite barrier case).

ELECTRON-PHONON INTERACTION

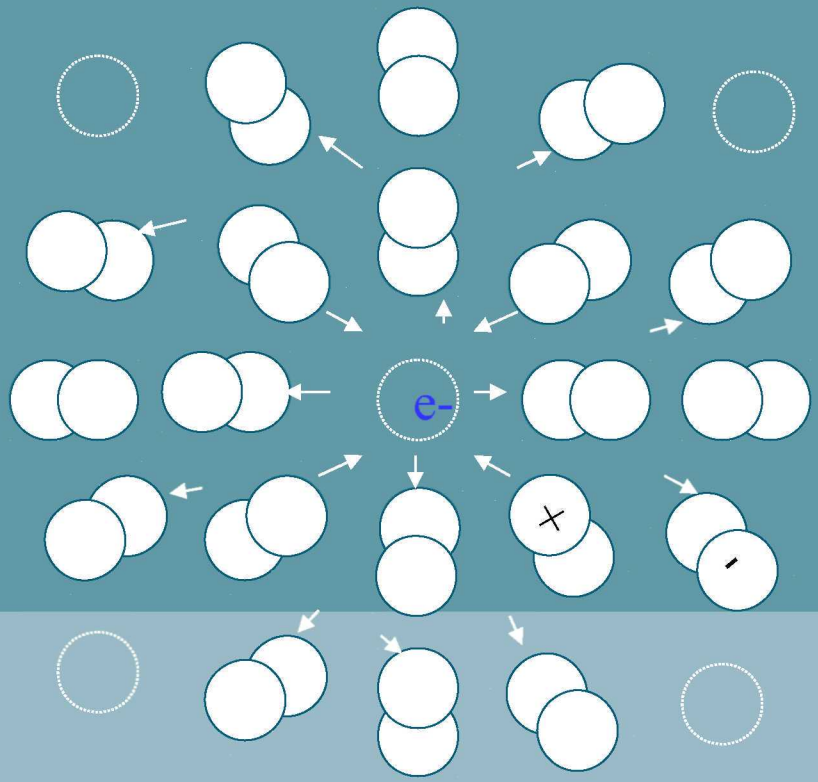

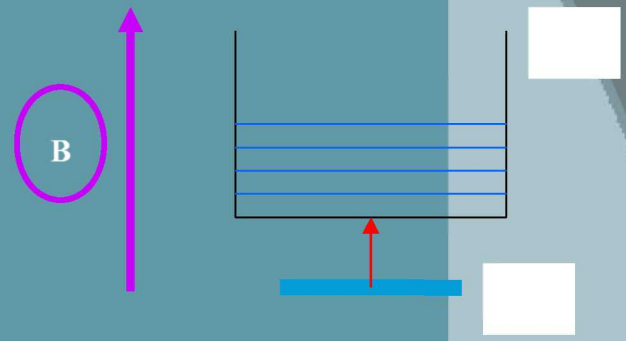

CuCl: $\alpha_0 = 2.45$

	III-V			II-VI		
	GaAs	GaP	InSd	**CdTe**	**ZnSe**	ZnS
α_0	0.067	0.201	0.023	0.315	0.448	0.694

Constant Couplage

$$\alpha_0 = \frac{1}{2}\frac{e^2/(\hbar/2m^*\omega_0)^{1/2}}{\hbar\omega}\left(\frac{1}{\varepsilon_\infty}-\frac{1}{\varepsilon_0}\right)$$

$$H = H_e + H_{LO} + H_{e-LO} + H_{ion-LO}$$

$$H_e = \frac{1}{2m_e^*}\left(\vec{p} + \frac{e}{c}\vec{A}\right)^2 - \frac{e^2}{\varepsilon_\infty r} + V(r)$$

$$H_{LO} = \sum_q \hbar\omega_{LO}\, a_q^+ a_q$$

$$H_{e-LO} = -\sum_{qlm} V_l(q_l)\, j_l(q_l r_e)\, Y_{lm}(\theta,\varphi)\, a_{lm}(q_l) + hc$$

$$H_{ion-LO} = \sum_{qlm} V_l(q_l)\, j_l(0)\, Y_{lm}(\theta,\varphi)\, a_{lm}(q_l) + hc \qquad V_l(q_l) = \left(\frac{4\pi e^2 \omega_{LO}}{J_{l+1/2}^2(q_l R) R^3 q^2}\right)\left(\frac{1}{\varepsilon_\infty} - \frac{1}{\varepsilon_o}\right)$$

Platzman Transformation

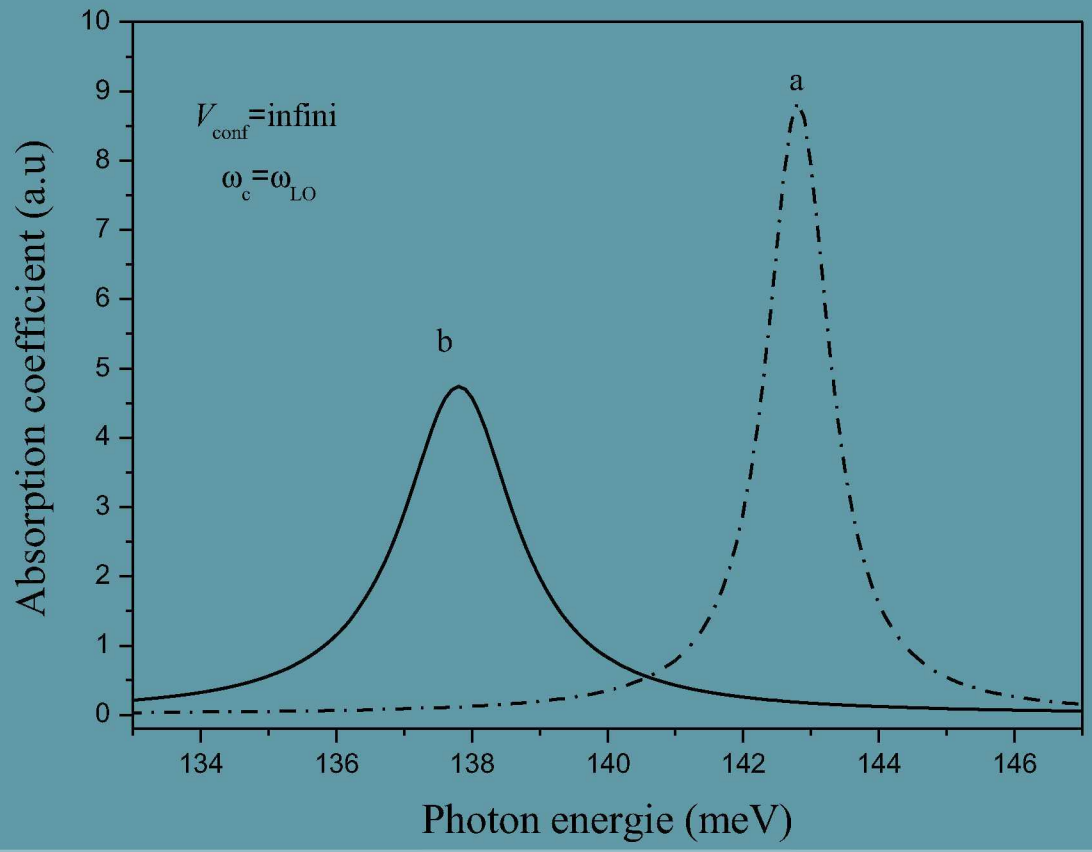

The absorption coefficient as a function of photon energy without polaron effects curve (a) and with polaron effects curve (b) (infinite barrier case).

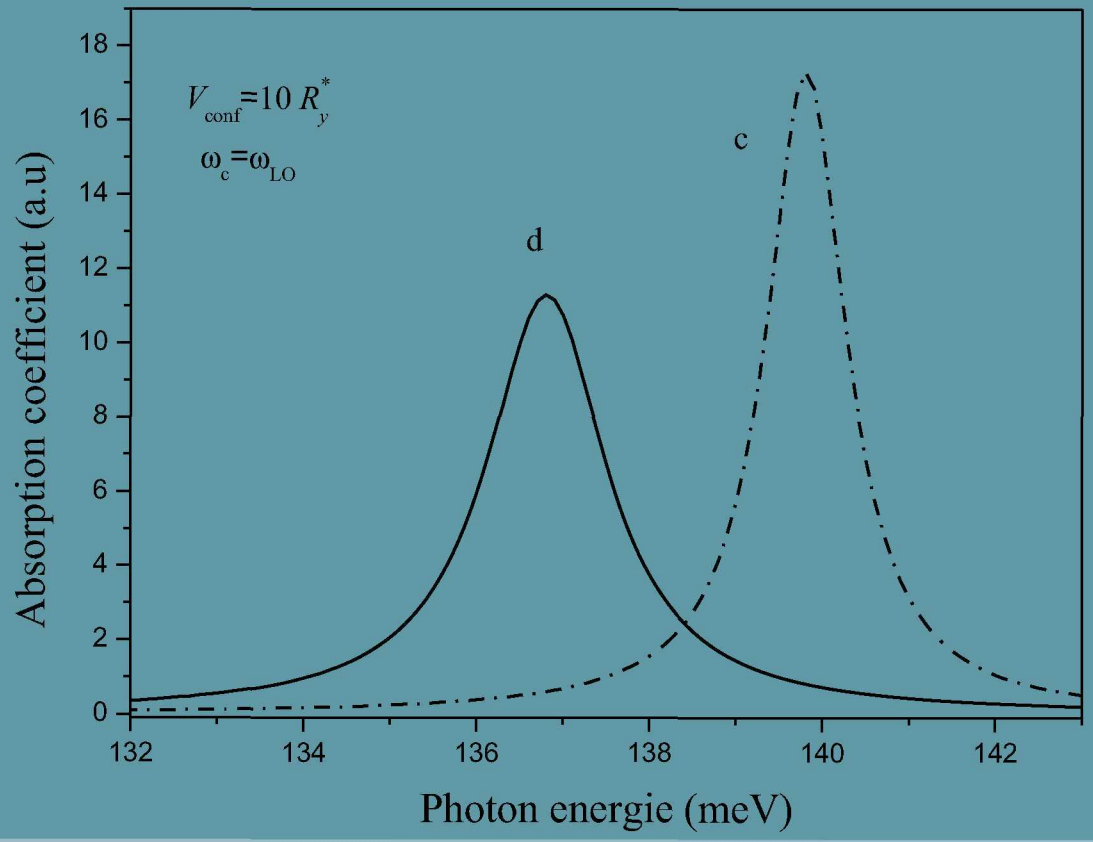

The absorption coefficient as a function of photon energy without polaron effects curve (c) and with polaron effects curve (d) (finite barrier case).

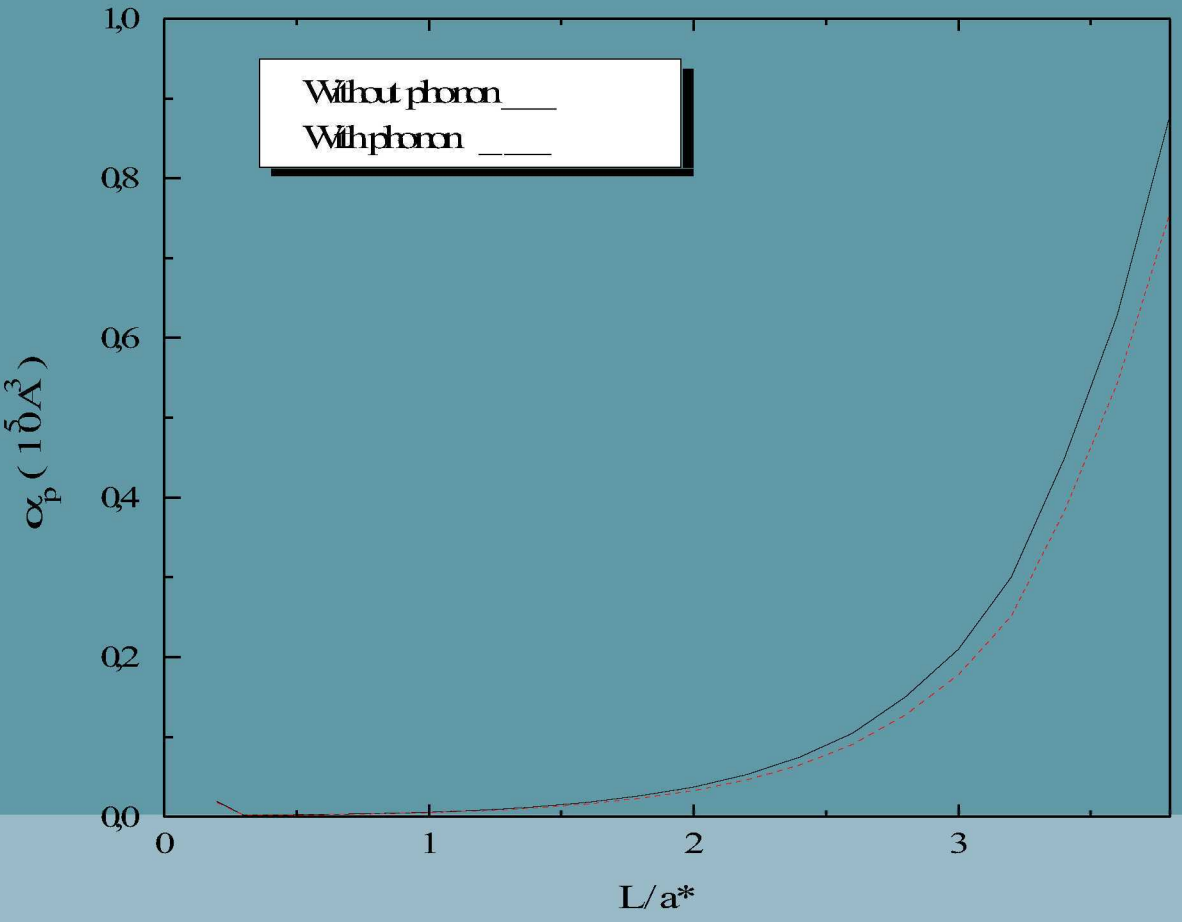

Polarisabilité α_p as a function of wire width with (dashed line, α_0=0.448) And without (solid line, α_0=0) the polaronic effects.

Quantum Well Wire

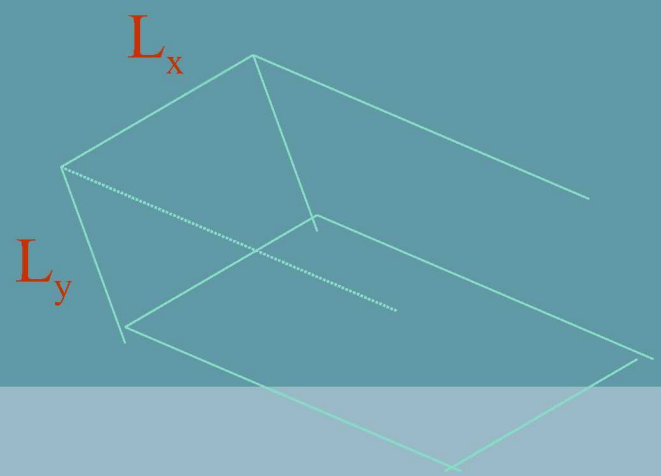

CuCl

$m^* = 0.5\ m_e$

$\varepsilon_0 = 7.9$

$R^* = 109$ meV

$a^* = 8.36$ Å

$\alpha_0 = 2.45$

BOUND POLARON

$$H_i = H_e + H_{ph} + H_{e-ph}$$

$$H_e = -\nabla^2 - \frac{2}{r} + V(x,y) + \gamma L_z + \frac{1}{4}\gamma^2\left(x^2 + y^2\right)$$

$$V(x,y) = \begin{cases} 0 & pour\ |x| \le \frac{l_x}{2}, |y| \le \frac{l_y}{2} \\ \infty & ailleurs \end{cases}$$

$$H_{ph} = \sum_q \hbar\Omega a_q^+ a_q$$

$$H_{e-ph} = \sum_q \left[V_q^* a_q^+ \exp\left(-i\vec{q}.\vec{r}\right) + V_q a_q \exp\left(i\vec{q}.\vec{r}\right)\right]$$

$$V_q = -\frac{i\hbar\Omega}{\sqrt{v}}(4\pi\alpha_0\tau_0)^{\frac{1}{2}} \qquad \tau_0 = \left(\frac{\hbar}{2m^*\Omega}\right)^{\frac{1}{2}}$$

$$H_i|\Psi_i\rangle = E_i|\Psi_i\rangle$$

$$|\Psi_i\rangle = |1s\rangle \exp\left[\sum_q (g_q a_q^+ - g_q^{\bullet} a_q)\right]|0\rangle$$

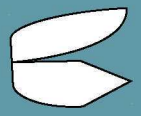

$$|1s\rangle = N\,Cos(K_1 x)\,Cos(K_2 y)\exp\left[-\left(\frac{x^2-y^2}{8b^2}+\frac{z^2}{8a^2}\right)\right]$$

$$E_i = E_0 + E_{ph} \qquad E_i = \langle\Psi_i|H_i|\Psi_i\rangle_{[a,b]}$$

FREE POLARON

$$|\psi_f\rangle = |f\rangle e^{s_1} e^{s_2} |\{n_q\}\rangle$$

$$|f\rangle = \frac{1}{\sqrt{\mathrm{L}}}\frac{1}{\sqrt{L_x L_y}}\cos(k_{nx}x)\cos(k_{ny}y)\exp(ik_z.z)$$

$$S_1 = -i\sum_q q_z . z . a_q^+ a_q$$

$$S_2 = \sum_q (f_q a_q^+ - f_q^* a_q)$$

$$\alpha(\omega) = \frac{4\pi^2}{n}\frac{e^2}{\hbar c}\frac{256 a^5 I'^4_{xx}}{l^2 I_{xx}^2 \sqrt{\pi}} \times \exp(-A)\{E_0\sqrt{E_0}x\sqrt{x-1}\exp[-4E_0 a^2(x-1)] +$$

$$A E_0'\sqrt{E_0'}x'\sqrt{x'-1}\exp[-4E_0' a^2(x'-1)]\}$$

$$x' = x - \frac{\hbar\Omega}{E_0} \qquad E_0' = E_0 - \hbar\Omega \qquad x = \frac{\hbar\omega}{E_0} \qquad E_0 = E_f - \frac{\hbar^2 k_z^2}{2m^*} - E_i$$

Figure. I

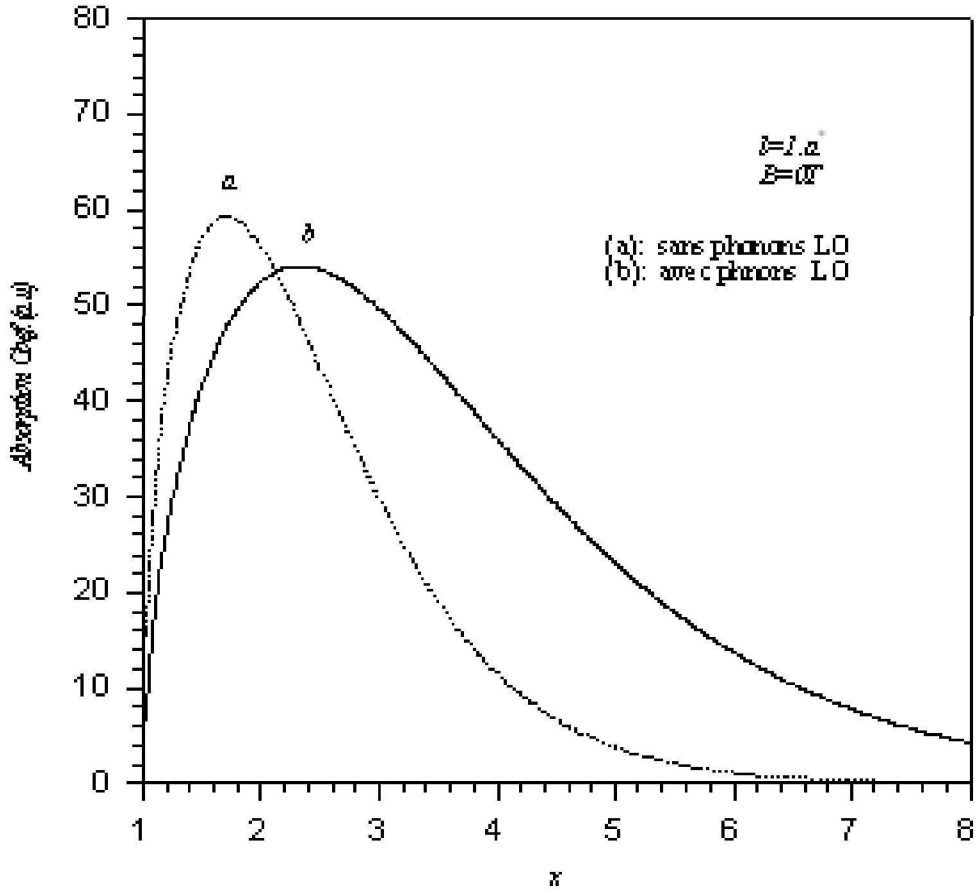
80
70
60
50
40
30
20
10
0
1
2
3
4
5
6
7
8
x
a
b
(a): sans phonons LO
(b): avec phonons LO

Figure. II

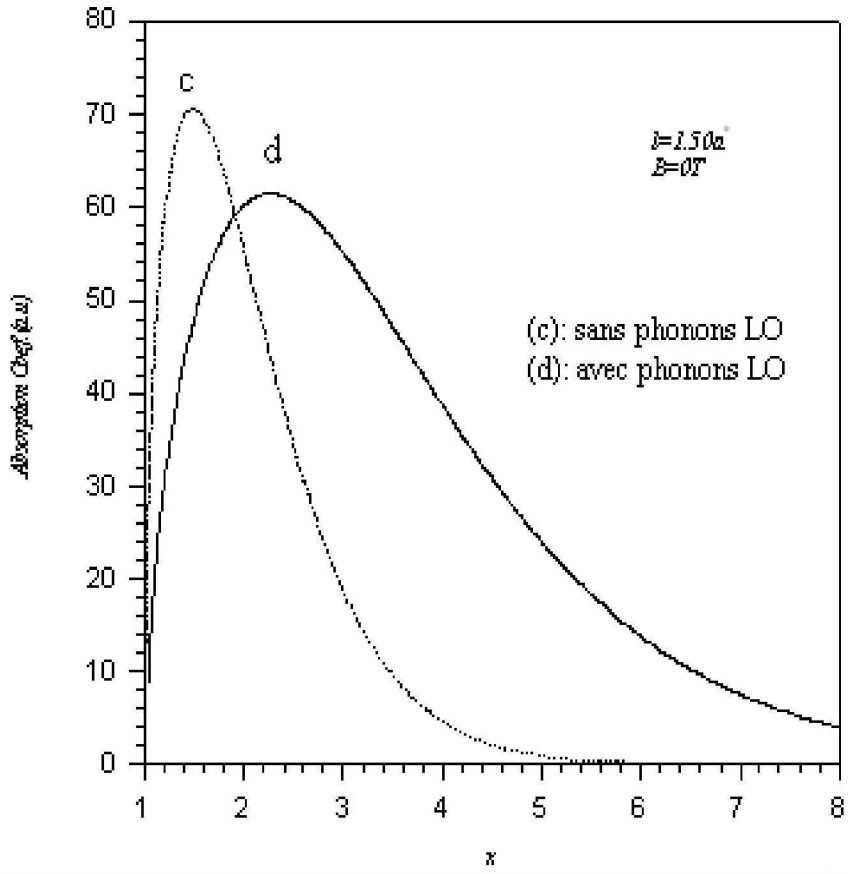
80
70
60
50
40
30
20
10
0
1
2
3
4
5
6
7
8
c
d
L=1.50a
B=0T
(c): sans phonons LO
(d): avec phonons LO
x

DIRECT AND INDIRECT BAND GAP

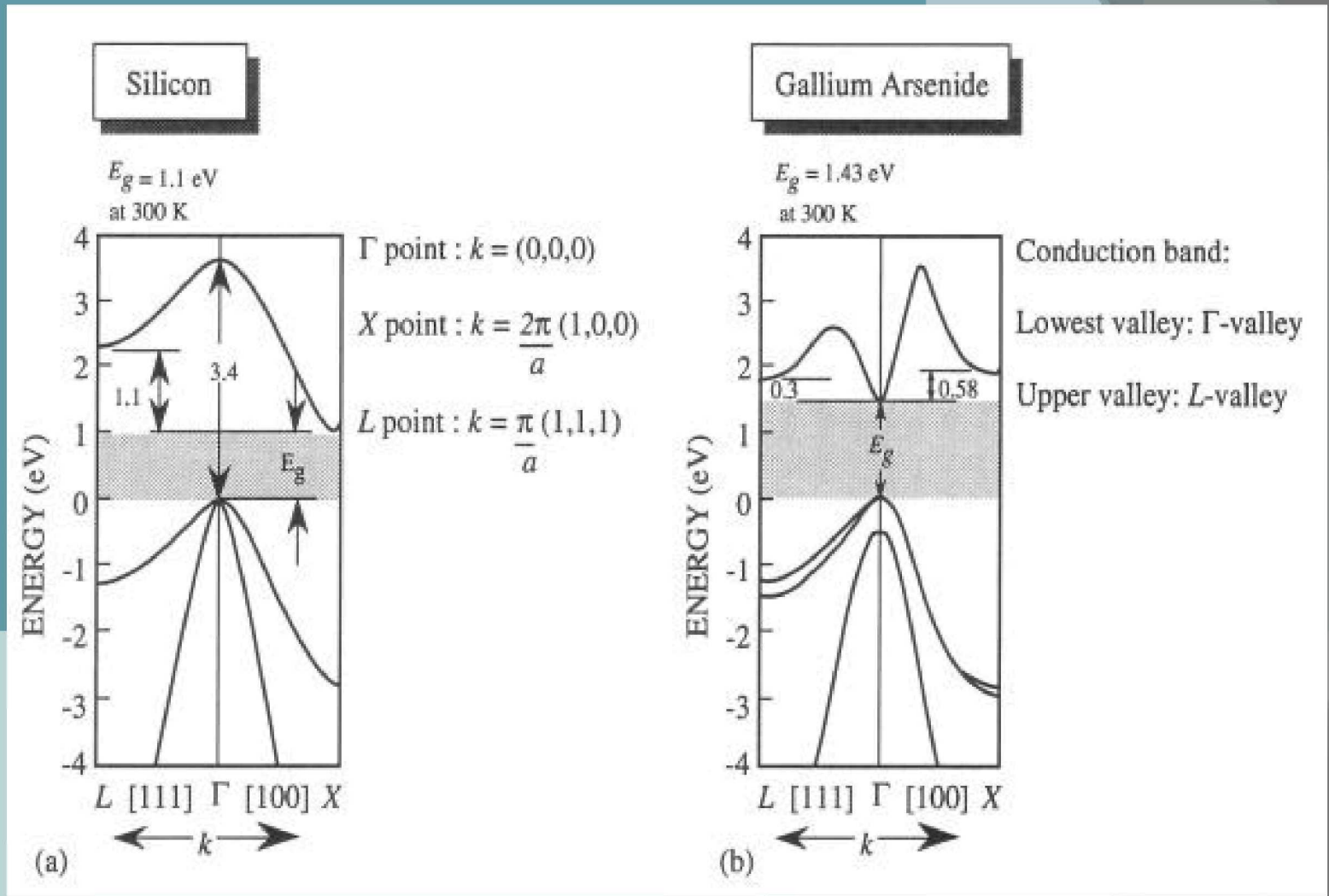

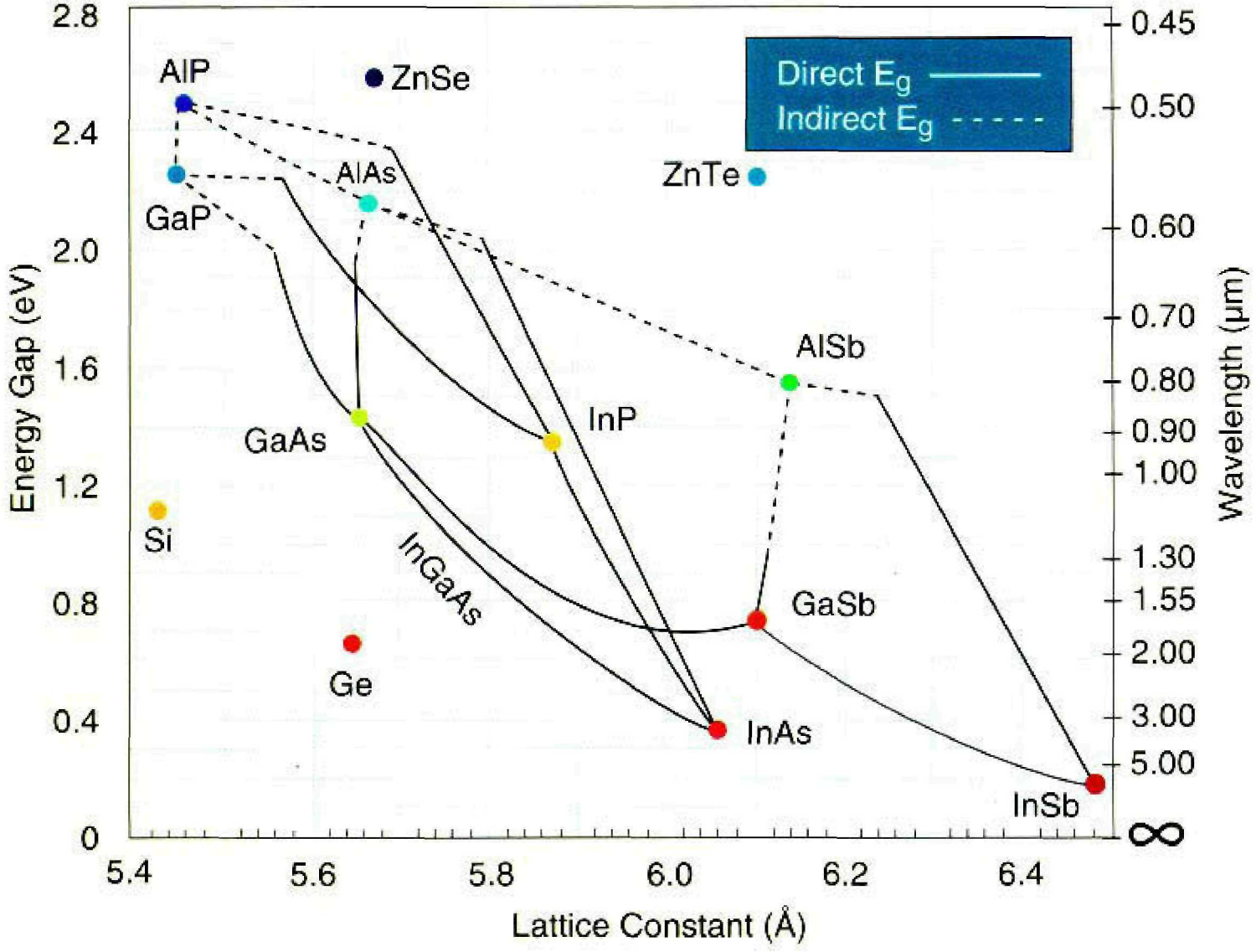
Direct E_g
Indirect E_g
AlP
ZnSe
AlAs
ZnTe
GaP
AlSb
InP
GaAs
Si
InGaAs
GaSb
Ge
InAs
InSb
Energy Gap (eV)
Wavelength (μm)
Lattice Constant (Å)
2.8
2.4
2.0
1.6
1.2
0.8
0.4
0
0.45
0.50
0.60
0.70
0.80
0.90
1.00
1.30
1.55
2.00
3.00
5.00
∞
5.4
5.6
5.8
6.0
6.2
6.4

Which materials?

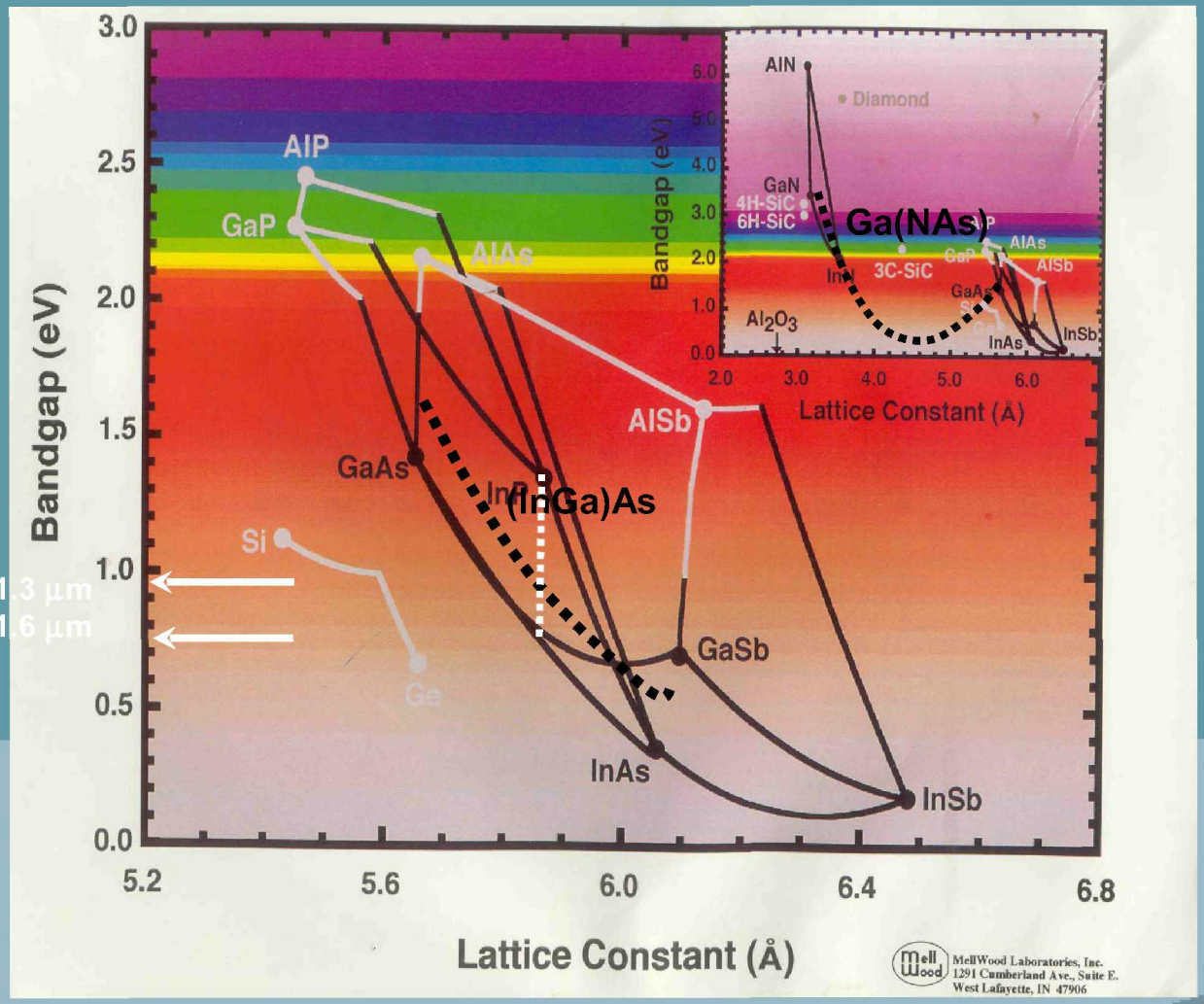

Old technology

Lattice matched

(GaIn)(AsP) on InP

New technology

Lattice mismatched

(GaIn)As on GaAs

Ga(NAs) or (GaIn)(NAs) on GaAs

Long wavelength QD-Lasers: roadmap

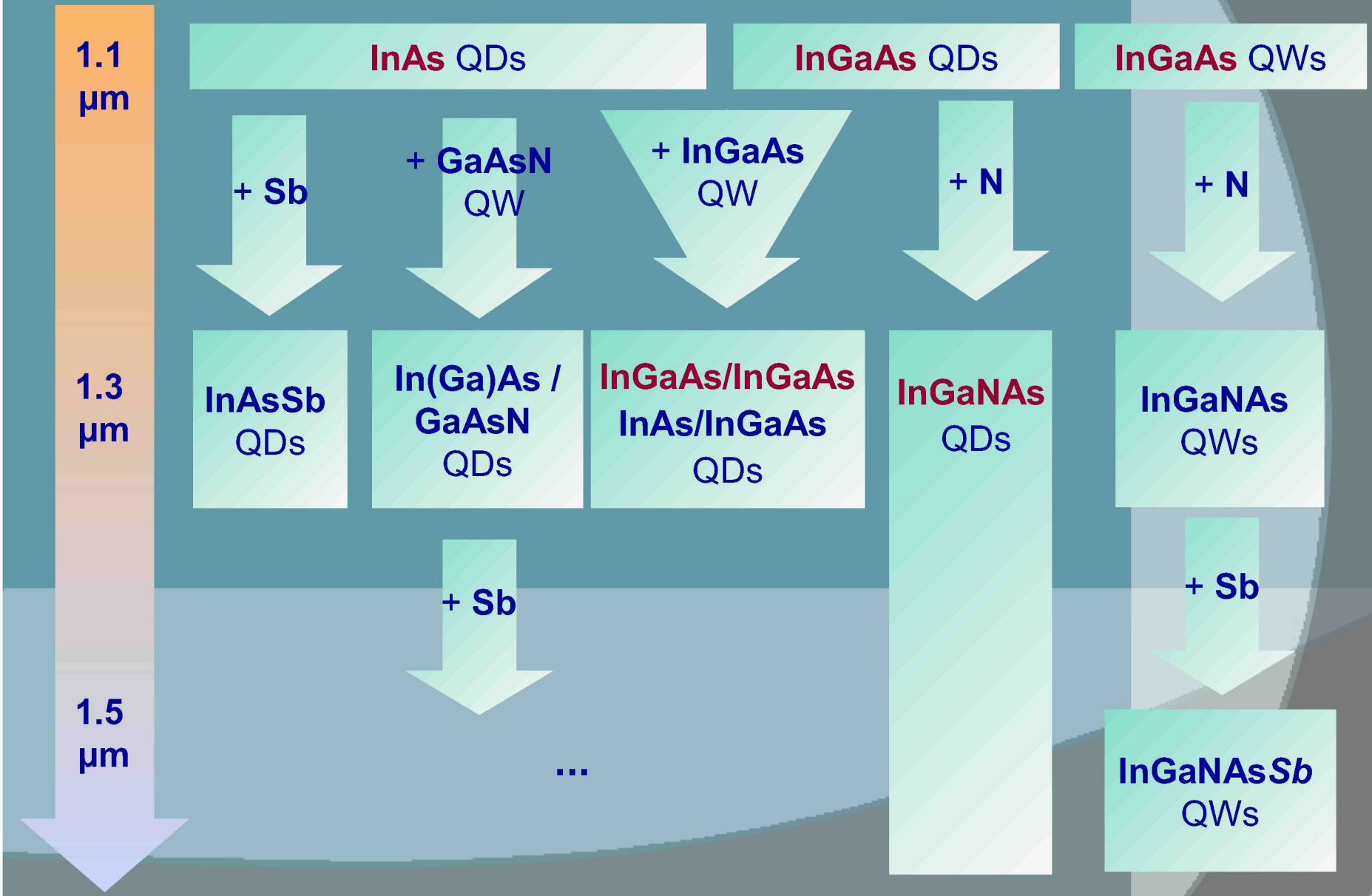

Conclusions

- The 1s-2p+ transition energy increases as function of the magnetic field and the 1s-2p- transition energy may be increased or decreased as function of competion between the magnetic and geometric confinements.

- As a consequence, of the scaling laws the absorption coefficient varies systematically as a function of quantum dot size.

- The application of the magnetic field induced reduction of the absorption peak and a displacement of the threshold energy.

Summary

- Discrete energy levels, artificial atom
- Making better lasers
- Lots of room for further research!

Do it with Dots !

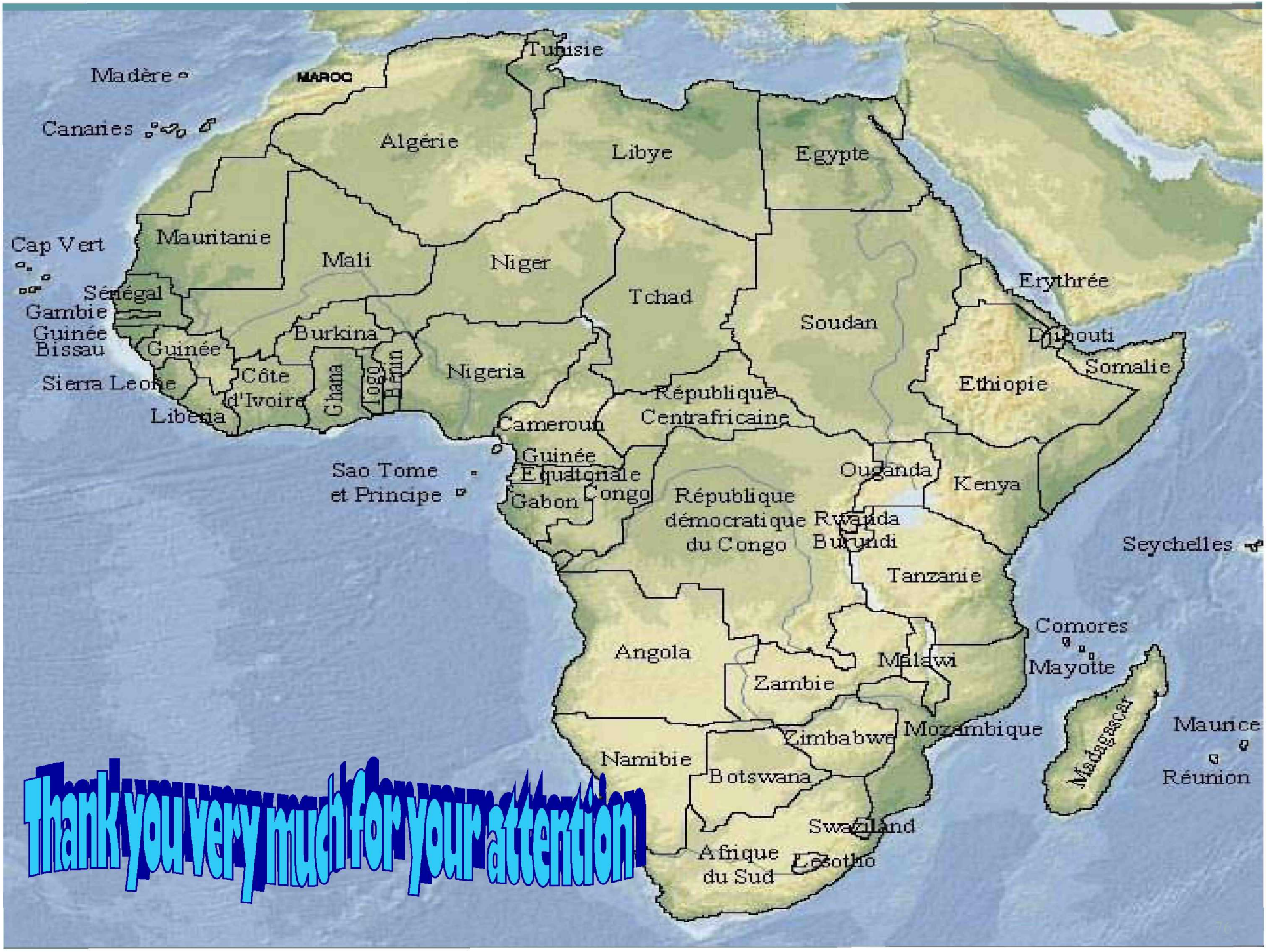

Thank you very much for your attention